ACS PHYSICAL CHEMISTRY Au
AN OPEN ACCESS JOURNAL OF THE AMERICAN CHEMICAL SOCIETY

pubs.acs.org/physchemau
Article

Investigation of Corrosion Inhibition of Mild Steel in 0.5 M H_2SO_4 with *Lachancea fermentati* Inhibitor Extracted from Rotten Grapefruits (*Vitis vinifera*): Adsorption, Thermodynamic, Electrochemical, and Quantum Chemical Studies

Baluchamy Tamilselvi, Durvas Seshian Bhuvaneshwari,* Periyakaruppan Karuppasamy,* Sethuramasamy Padmavathy, Santhosh Nikhil, Surendra Boppanahalli Siddegowda, and H C Ananda Murthy*

Cite This: *ACS Phys. Chem Au* 2024, 4, 67−84

ABSTRACT: Corrosion inhibition of mild steel (MS) was studied using *Lachancea fermentati* isolate in 0.5 M H_2SO_4, which was isolated from rotten grapes (*Vitis vinifera*) via biofilm formation. Biofilm over the MS surface was asserted by employing FT-IR and FE-SEM with EDXS, electrochemical impedance spectroscopy (EIS), AFM, and DFT-ESP techniques. The weight loss experiments and temperature studies supported the physical adsorption behavior of the corrosion inhibitors. The maximum inhibition efficiency (IE) value (90%) was observed at 293 K for 9×10^6 cfu/mL of *Lachancea fermentati* isolate. The adsorption of *Lachancea fermentati* isolate on the surface of MS confirms Langmuir's adsorption isotherm model, and the $-\Delta G$ values indicate the spontaneous adsorption of inhibitor over the MS surface. Electrochemical studies, such as potentiodynamic polarization (PDP) and EIS were carried out to investigate the charge transfer (CT) reaction of the *Lachancea fermentati* isolate. Tafel polarization curves reveal that the *Lachancea fermentati* isolate acts as a mixed type of inhibitor. The Nyquist plots (EIS) indicate the increase in charge transfer resistance (R_{ct}) and decrease of double-layer capacitance (C_{dl}) values when increasing the concentration of *Lachancea fermentati* isolate. The spectral studies, such as UV−vis and FT-IR, confirm the formation of a complex between MS and the *Lachancea fermentati* isolate inhibitor. The formation of biofilm on the MS surface was confirmed by FE-SEM, EDXS, and XPS analysis. The proposed bioinhibitor shows great potential for the corrosion inhibition of mild steel in acid media.

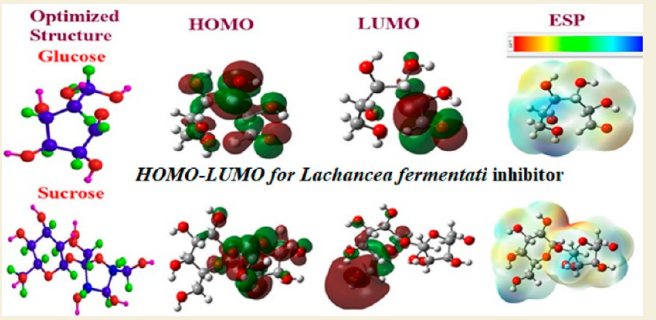

KEYWORDS: *Lachancea fermentati isolate, mild steel, DFT study, temperature effect, biofilm formation, electrochemical techniques*

1. INTRODUCTION

Mild steel (MS) is a type of ferrous alloy that has extensive usage, especially in tanks used for petroleum refinement and storage. This metal has proximity to steel and is prone to corrosion in an acidic environment.[1−3] The corrosion inhibitor, which enables a reduction in the corrosion rate, involves several methods. The chief methods practiced in controlling corrosion under corrosion inhibition include protection coating, inspection and monitoring of tools and materials, passivation, metal plating, frequent painting, and forming biofilm.[4,5] The use of corrosion inhibitors, particularly green substances, has become an area of keen research interest. Under this approach, ecofriendly corrosion inhibitors are developed, although it is true that green inhibitors extracted from plant sources are popularly known for their corrosion prevention potential. By this, corrosion mitigation is evoked by the deterioration of mild steel and enhanced malleability and formability within the acidic medium.[6−8] Quite differently, a biofilm is a unique and salient method for reducing corrosion in mild steel. This is evident from its characteristics, such as being environment-friendly, less hazardous, and biodegradable under optimal ecological conditions.[9]

The biofilm formation using microbes on metal surfaces has better potential than expensive paints and involves frequent faces in ordinary environments, pharmaceuticals, and engineering fields. On research platforms, microbes have created much interest in corrosion.[10] As per the recent findings, biofilm

Received: September 28, 2023
Revised: October 24, 2023
Accepted: October 24, 2023
Published: December 8, 2023

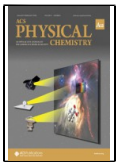

https://doi.org/10.1021/acsphyschemau.3c00055
ACS Phys. Chem Au 2024, 4, 67−84

extends various benefits to different industrial applications apart from corrosion inhibition, bioremediation,[11] industrial wastewater remediation,[12] quorum sensing,[13] and plant protection.[14,15] Biofilms are a pool of microorganisms that exist cumulatively and are attached to multipart surfaces by passing through a self-produced polymer matrix. Under normal conditions, a bacterial biofilm is formed from bacterial cells available within the EPS (extracellular polymeric substance), which allows for the amalgamation of the entire growing community. This is extended to the substrate at the metal−liquid interface or mixing of yeast, fungi, algae, and protozoa for a better report with additional biotic or abiotic surfaces.[16] This is the most important property of microbes in the formation of biofilm on metal surfaces and has been recognized.[17]

In recent decades, numerous reports were published for the formation of biofilm on the inhibition of metal corrosion. Many bacteria, such as *Bacillus* and *Pseudomonas* strains, have been used for the corrosion inhibition of metals. *Pseudomonas S9* and *Serratia marcescens EF190* cultures were used to inhibit the corrosion of the SIS 1146 steel.[18−20] The mild steel corrosion inhibition was studied, and the result revealed that the 2 to 10-fold excess of mild steel corrosion inhibition was achieved because of *Pseudomonas fragi* and *Escherichia coli DH5a* (pKMY319) biofilms. The aerobic biofilm formation has proved its corrosion inhibition toward metals compared with sterile controlled cultures. Biofilms are not only formed by bacterial strains but also yeast, which has characteristic features for corrosion inhibition from biofilm formation. In addition, the yeast biofilm structures are more complex to wipe out through the effect of antifungal agents. Furthermore, *Aspergillus*, *Cryptococcus*, *Coccidioides*, and *Pneumocystis* fungi also form biofilms.[21] Among all biofilms formed by microbes, the formation of biofilm by yeast is one of the extremely structured biofilms attached to the surface of the materials.[22] The biofilm by yeast cells in food was documented and it sticks on very easily in biotic, as well as abiotic, surfaces because of hydrophobic interactions.[23,24] The yeast cells are stuck onto the surface (plastic and stainless steel), develop network arrangements via hyphae/pseudohyphae, and accumulate an extracellular matrix. Yeast cells are potential candidates for the formation of network structure on the surface of materials and the *pseudohyphae* was associated in the biofilm. The reported research works revealed that yeast cells have a variety of properties, such as enzymatic activities, cohesiveness, adhesive nature, nutritional foundations, protection, and mechanical properties.[25] The biofilm (*Pichia* spp. and *Candida* spp.) formation was observed in olive oil and it showed excellent control on the fermentation of olive.[26] The immersion of metal in fluid circumstances creates a formation of biofilm on the metal surface via a biofilm matrix, and it decreases the reactions between the corrosive agent and the metal by making a transport barrier. As a result, the corrosion penetration rate was decreased because of less interaction between metal and corrosive agent.[26,27] Many well-known isolates (*Dikarya, Ascomycota, Saccharomycotina, Saccharomycetes, Saccharomycetales, Pichiacea*, and *Pichia* sp.) for the secretion of yeast in optimum environmental circumstances.[28,29] Among the aforementioned isolates, *Pichia* sp. isolate received much focus for inhibition of mild steel corrosion in environmental conditions because of the biofilm formation over the surface of mild steel compared with other yeasts.[30,31] The formation of biofilm due to microbes is complex because of extracellular polymeric substances and it offers the protection of biofilms under optimum environmental conditions.[32] The bacterial cells have the potential to attach on the surface of the metals, polymers, and materials because of the formation of mature biofilms.[33] Many bacterial pathogens have been reported, such as *P. aeruginosa, Klebsiella pneumoniae, A. baumannii, Pseudomonas aeruginosa*, and *Enterobacter* spp. *K. pneumoniae* for the formation of protective layer/biofilm on the surface of the materials.[34] Thus, the development of biomaterials to inhibit the corrosion of materials through the formation of biofilm on the surface is an emerging trend.[35] The iron(III)−salen complex was tested against the four pathogenic bacterial strains, and the result exhibited excellent inhibition potential against Gram-negative, as well as Gram-positive, bacterial strains because of the adsorption of iron(III)−salen complex on the surface of the cell wall of the pathogenic bacterial strains.[36]

Nowadays, biofilms of *Lachancea fermentati* spp., *Saccharomyces cerevisiae* yeast, and *Lachancea thermotolerans* spp. are used for biofilm formation in sour beer or low-alcohol beer[37] and alcohol maturation and fermentation.[38] The formation of biofilm on the metals begins after immersing the metal into the liquid state, and there is a hitch from the biofilm environment by which the transportation is affected to prevent the corroded agents.[39] The familiar isolates, such as *Saccharomycetes, Saccharomycetales, Saccharomycetaceae, Ascomycota, Saccharomycotina, Dikarya, Lachancea*, and *Lachancea fermentati*, are used to secrete yeast under suitable ecological conditions.[40] In addition, the *Lachancea fermentati* isolate possesses the potential to spin out structural modifications that could be below environmental conditions. Such conditions are quite suitable for the production of biofilm by the isolates on the metal surfaces.[41]

The present work focuses on the investigation of the corrosion prevention of mild steel by *Lachancea fermentati* isolate, which is derived from different varieties of rotten grapes, in a 0.5 M H_2SO_4 solution under optimal experimental conditions. On the basis of the literature survey, it is established that the *Lachancea fermentati* biofilm test for corrosion inhibition potential is conducted for the first time as a research activity. Various techniques have been employed, such as weight loss, electrochemical, FT-IR, FE-SEM with EDXS mapping analysis, AFM, and quantum chemical calculations, for the study of the adherence and corrosion inhibitive nature of the *Lachancea fermentati* isolate with mild steel. The obtained results revealed that the inhibitor used in this study acts as a cost-effective, environmentally sustainable bioinhibitor, and this research study paves a new approach for controlling mild steel corrosion in acid media.

2. EXPERIMENTAL SECTION

2.1. Collection of Samples

Black grapes were used to isolate yeast strains, which were purchased from household fruit shops in and around Madurai city and collected using sterile polypropylene (PP) bags for the sake of preserving their freshness. These fruits were kept in a refrigerator and immediately brought to the laboratory at 4 °C until further processing.

2.1.1. Media Used. The culture medium preferred for the isolation of the yeast strain was Yeast Extract Peptone Dextrose Agar (YPD) with the following components: 10 g/L of yeast extract, 10 g/L of peptone, and 20 g/L of agar with 20 g/L of glucose. YPD medium appendages with 30 mg/mL of chloramphenicol or erythromycin were used for yeast strain isolation.

https://doi.org/10.1021/acsphyschemau.3c00055
ACS Phys. Chem Au 2024, 4, 67−84

Scheme 1. Yeast Isolation Method from Black Grapes

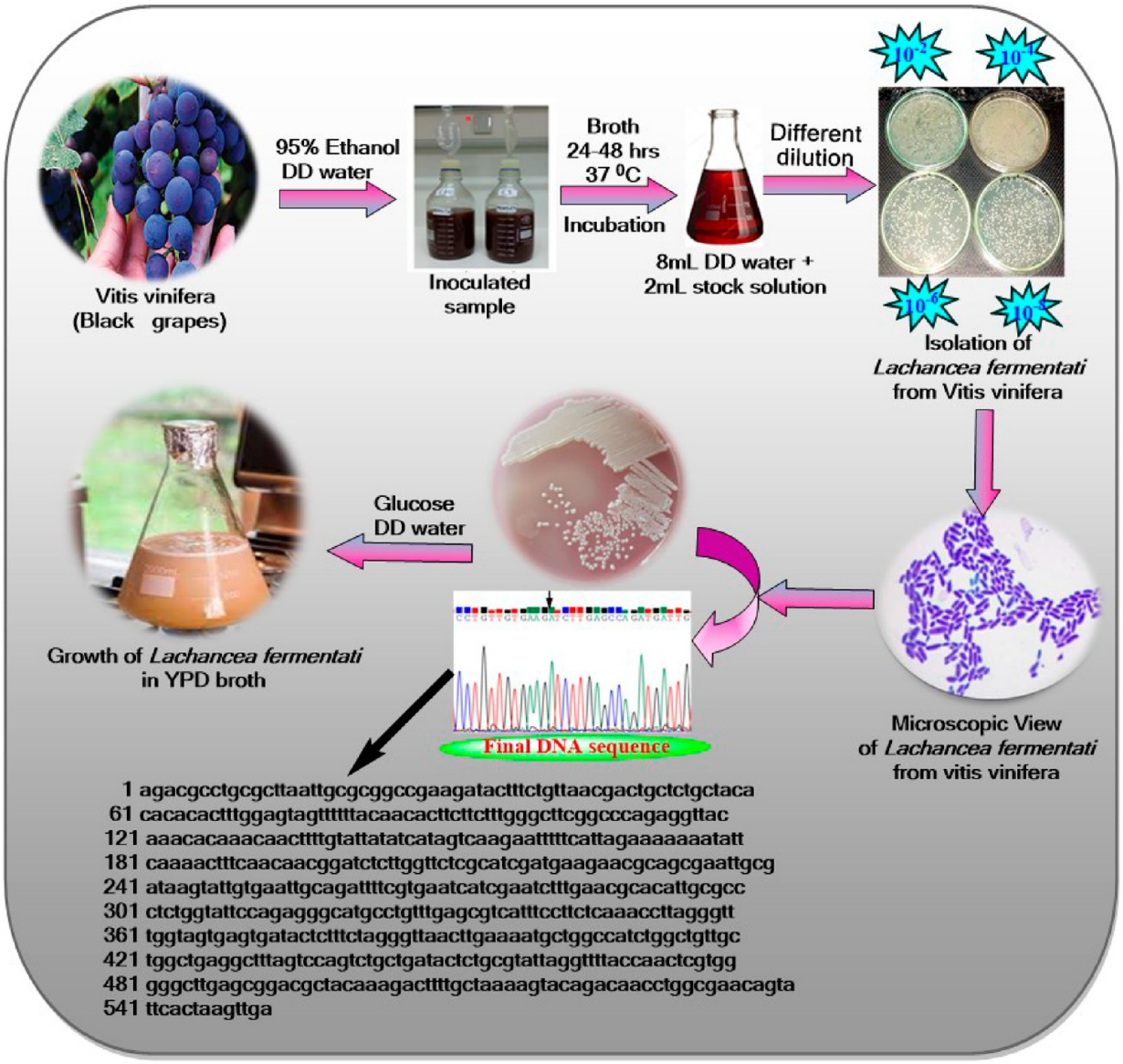

2.2. Techniques Used

2.2.1. Yeast Isolation Technique. The seclusion of yeasts from grapes was done by surface sterilization in 95% ethanol and then washing in distilled water. For incubation, the as-prepared YPD samples were supplemented on the broth for 2 days at 37 °C. After the incubation, approximately 1.5 mL of broth was diluted and spread on the plated YPD agar with appendages of about 30 mg/mL of erythromycin or chloramphenicol. The plates were intended for subsequent incubation for 2 days at 37 °C, as depicted in Figure S1a. Then, the colonies were chosen on the basis of color and colony morphology and purified further by employing plating on fresh YPD under similar conditions. Thus, the colonies were isolated from grown YPD samples and conserved in suitable YPG tubes by 4 °C, as shown in (Scheme 1).[42]

2.2.2. Yeast Isolate Identification. Under high-power resolution using compound microscopes, the strains of yeast were confirmed when the cells were stained with methylene blue (MB). Similarly, when the yeast cells were observed during germination, they were budding. After that, the yeast cells were put for separate inoculation into freshly prepared glucose water for further incubation for 2−3 h at 37 °C. Consequently, wet volumes of the cell cultures were prepared and observed under the microscope to confirm the budding of yeast cells.

2.2.3. Isolate Characterization. On the basis of their effectiveness in corrosion inhibition studies, the selected yeast isolates were identified by the 18S rRNA sequencing method. The characterization at the molecular level was done for the selected yeast isolates derived from biofilm attachment results at Optimurz Biosolutions in Chennai, and the results were confirmed by sequence analysis. The recovered 18S rRNA sequences from isolates were compared with those in the available literature database. The obtained isolate nucleotide sequence results were well-matched with *Lachancea fermentati* (accession number MH476356.1) and stored in the GenBank database (Figure S1b). The details of the identification by DNA sequencing were explained clearly in the Supporting Information.

2.2.4. Preparation of Yeast Isolate Samples for Corrosion Inhibition Study. Enrichment of yeast isolates was performed utilizing the colonies upon the addition of 50 mL of sterile yeast peptone dextrose (YPD) broth with 30 mg/mL of erythromycin or chloramphenicol under incubation conditions at 28 °C overnight.[43] Finally, the corrosion inhibition efficiency (IE %) values of the yeast isolates were determined for the resultant samples.

https://doi.org/10.1021/acsphyschemau.3c00055
ACS Phys. Chem Au 2024, 4, 67−84

2.2.5. Preparation of Electrode Specimens and Acid Electrolytes. The mild steel with a chemical composition of carbon (0.13%), sulfur (0.04%), silicon (0.18%), phosphorus (0.39%), copper (0.025%), and the remaining percentage of Fe, with dimensions of 2.5 cm × 2.5 cm × 0.5 cm, was used as a working electrode. The aforementioned dimensions of the mild steel specimens were polished well with various grades (400−800) of emery papers. Then, the polished mild steel surface was washed with deionized water and acetone and masked with Teflon tape. The remaining unmasked mild steel surface was considered to be an exposed area (0.25 cm^2) in the electrochemical study.

2.2.6. Temperature Studies. The effect of temperature on the corrosion inhibition of mild steel with and without *Lachancea fermentati* isolates between 293 and 313 K was studied in 0.5 M H_2SO_4. The low-temperature study was done by using instruments in a cryostatic bath under ice-cooled conditions. This process enabled the employment of *Lachancea fermentati* isolate inhibitors for mild steel corrosive environments at different concentrations. The influence of immersion time was carried out for 2 h followed by rinsing of the MS specimens with deionized water and acetone. In addition, weight loss measurements were carried out according to standard procedure (ASTM G31−03).[44] Furthermore, the mild steel specimens were weighed accurately before and after immersion. The corrosion rate (mpy) and weight losses were calculated using eq 1 for various concentrations of *Lachancea fermentati* isolates.

$$\mathrm{CR(mpy)} = \frac{87.6 \times \Delta W}{\rho A T} \tag{1}$$

where CR denotes corrosion rate, ρ is the density of the MS specimen, ΔW is the change in weight (mg), A is the surface area of the MS specimen exposed to the electrolyte (cm^2), and T is the exposure time (hr). The inhibition efficiency (IE %) and surface coverage (θ) were evaluated from eqs 2 and 3.

$$\mathrm{IE}\ (\%) = \frac{W_0}{W_i - W_0} \times 100 \tag{2}$$

$$\theta = \frac{W_0}{W_i - W_0} \tag{3}$$

where W_0 and W_i are the MS weight losses (in mg) in the absence and presence of *Lachancea fermentati* inhibitors, respectively

2.2.7. Electrochemical Measurement. The electrochemical study was performed using a CHI660E (CH-instrument, USA) in a thermostated cell. This component was composed of a three-electrode system, which consists of a working electrode [exposure area (1 cm × 1 cm) of the MS specimen], a reference electrode [Ag/AgCl (saturated KCl)], and an auxiliary electrode (a platinum sheet). All of the electrochemical measurements were conducted in this process, and the MS electrode was made to contact a corrosive medium for 30 min. This time-bound task was made for obtaining steady-state conditions and attaining the stable open circuit potential (OCP) value before starting each experiment. An electrochemical impedance spectroscopy study was carried out between the frequency ranges of 100 kHz and 0.1 Hz at constant OCP and a 5 mV/s value of peak−peak amplitude. The electrochemical impedance spectroscopy (EIS) data, including double-layer capacitance (C_{dl}) as well as charge transfer resistance (R_{ct}), were evaluated from Nyquist plots, and an equivalent circuit was formulated based on the best-fitting EIS data. The corrosion inhibition efficiency was calculated using eq 4.

$$\mathrm{IE}\ (\%) = \mathrm{R_{ct(inh)}} - \mathrm{R_{ct(blank)}/R_{ct(inh)}}(\%) \tag{4}$$

where $R_{ct(blank)}$ and $R_{ct(inh)}$ denote the charge transfer resistance in the absence and presence of *Lachancea fermentati* inhibitors for the corrosion inhibition of MS specimens in 0.5 M H_2SO_4. For the potentiodynamic polarization study, a potential of −300 and +300 mV (Ag/AgCl as reference electrode) with 0.333 mV s^{-1} scan rates starting from the cathodic and anodic directions were engaged. The evaluation of Tafel data was done using CHI660E software by extrapolating the Tafel lines to their points of intersection. Through this method, the following Tafel data could be evaluated: corrosion current density (i_{corr}), corrosion potential (E_{corr}), anodic slope (β_a), and cathodic slope (β_c) values. The electrochemical corrosion inhibition efficiency (IE %) was calculated using corrosion current density (i_{corr}) values in the absence and presence of *Lachancea fermentati* inhibitors by applying eq 5.

$$\mathrm{IE}\ (\%) = i_{\mathrm{corr\ (blank)}} - i_{\mathrm{corr\ (nhi)}}/i_{\mathrm{corr\ (blank)}}(\%) \tag{5}$$

where $i_{corr\ (blank)}$ and $i_{corr\ (inh)}$ are corrosion current densities for uninhibited, as well as inhibited, surfaces of MS specimens.

2.2.8. Spectral and Analytical Characterizations Study. The structural characteristics of the scratched MS film were investigated using FT-IR spectroscopy with the solid KBr pellet method on an FT-IR instrument model SHIMADZU-8400S. The absorption characteristics were studied for a corrosive medium (before and after immersion in MS) using a JASCO (V-560) model spectrophotometer. The morphological changes on the MS surface in the absence and presence of inhibitor were investigated by FESEM-EDXS [Zeiss Sigma FE-SEM with a Gemini column (USA), EDX-BRUKER, Nano X Flash detector 5030 (Germany), and AFM (Nanosurf EASY-SCAN2, Switzerland)] analysis.

2.2.9. Quantum Chemical Study. The quantum chemical study for the *Lachancea fermentati* isolate was performed using the Gaussian 09 (G00) software package ($DMol_3$) with B3YLP-6-31G and the DND basis set. Further, this examination was done to understand the structural insights of the *Lachancea fermentati* isolate using density functional theory (DFT).[45,46] The *Lachancea fermentati* isolate was put for optimization in the gas phase, restrained by Becke's three-parameter correlation functions. Also, the structural properties were evaluated using a hybrid correlation functional (Lee−Yang−Parr) in conjugation with a basis set [Pople 6-31G (d)].[47,48] This quantum chemical study provided the data of HOMO−LUMO details, band gap energy, electron affinity, electronegativity, hardness, dipole moment, ionization potential, softness, and electron transfer between the *Lachancea fermentati* isolate and MS surface, respectively.

3. RESULTS AND DISCUSSION

3.1. Weight Loss Measurements

The weight loss method was used to estimate the inhibitory potential of various concentrations of *Lachancea fermentati* isolates for the corrosion inhibition of MS specimens in 0.5 M H_2SO_4 solution. The experimental results obtained from this examination are depicted in Table 1, which clearly shows that the corrosion rate decreases, and inhibition efficiency increases because of the application of various concentrations of the *Lachancea fermentati* isolate in a 0.5 M H_2SO_4 solution. From Table 1, it was observed that the corrosion rate was extremely elevated when the temperature rose from 293 to 313 K. The obtained data are shown in Figure 1a,b. A reduction in corrosion rate occurred when *Lachancea fermentati* isolate concentration was increased, which revealed biofilm formation over the surface of MS. Subsequently, the formation of biofilm over the MS surface exhibits enhanced surface coverage and decreases the number of active sites, which is ideal for accessing the corrosion.[49] Similarly, there was a rise in the trend of IE (%) when the *Lachancea fermentati* isolate concentrations were increased, and the optimal/maximum IE (90.14%) was attained at *Lachancea fermentati* isolate concentrations of 9 × 10^6 cfu/mL. The optimal result was based on the resulting increase in the *Lachancea fermentati* isolate concentrations. Thus, an appreciable decrease in the IE (%) based on the optimal concentration of 9 × 10^6 cfu/mL could be achieved. Moreover, the addition of *Lachancea fermentati* isolate inhibitor concentrations exerts an influence on the contest between the molecules to adsorb on the MS

https://doi.org/10.1021/acsphyschemau.3c00055
ACS Phys. Chem Au 2024, 4, 67−84

Table 1. Corrosion Rate and Inhibition Efficiency Data from Mass Loss Measurement in 0.5 M H_2SO_4 with *Lachancea fermentati* Isolates

temperature (K)	concentration (10^6 × cfu/mL)	corrosion rate (mpy)	θ	IE (%)
293	0	1720.10		
	6	546.56	0.6822	68.22
	7	338.29	0.8033	80.33
	8	234.72	0.8635	86.35
	9	169.59	0.9014	90.14
	10	180.93	0.8948	89.48
298	0	2234.41		
	6	755.65	0.6618	66.18
	7	646.75	0.7105	71.05
	8	541.18	0.7578	75.78
	9	333.39	0.8508	85.09
	10	426.71	0.8090	80.90
303	0	3283.38		
	6	1277.91	0.6108	61.08
	7	1069.01	0.6744	67.44
	8	860.11	0.7380	73.80
	9	693.43	0.7889	78.89
	10	775.65	0.7637	76.37
308	0	3643.26		
	6	2046.18	0.4383	43.83
	7	1523.43	0.5818	58.18
	8	1098.56	0.6984	69.85
	9	968.34	0.7342	0.7342
	10	1225.36	0.6637	0.6637
313	0	3893.12		
	6	2357.23	0.3945	39.45
	7	1872.46	0.5190	51.90
	8	1589.52	0.5917	59.17
	9	1158.39	0.7024	70.24
	10	1421.40	0.6349	63.49

surface. As per experimental results, when diverse *Lachancea fermentati* isolate concentrations were used for 2 h, a prospective IE (%) could be obtained, and finally, it was reduced as a result of *Saccharomyces cerevisiae* degradation.[50]

3.2. Thermodynamic Data Evaluation

The evaluation of activation parameters is essential to analyze the interaction of the mild steel with the *Lachancea fermentati* inhibitor at the activation state in the acid medium. The mild steel corrosion inhibition study was carried out in 0.5 M H_2SO_4 at various temperatures (ranging from 303 to 313 K). The Arrhenius activation parameters were evaluated using eqs 6 and 7.[38]

$$\log(\mathrm{CR}) = \log(A) - \frac{E_a}{2.303RT} \tag{6}$$

$$\log(\mathrm{CR}/T) = \frac{R}{hN_A} + \frac{\Delta S^*}{2.303R} + \frac{\Delta H^*}{2.303RT} \tag{7}$$

where E_a denotes activation energy, A denotes frequency factor, R denotes gas constant, T denotes reaction temperature, N_A represents the Avogadro's number, ΔH denotes changes in enthalpy, and ΔS denotes changes in entropy at activation states.

The spontaneity of the adsorption process was confirmed with standard free energy of adsorption (ΔG_{ads}) values deduced from the Langmuir adsorption isotherm equation [($\Delta G_{ads} = RT \ln (55.5K_{ads})$], ΔH_{ads} values were calculated from the Van't Hoff equation, and change in entropy of adsorption was calculated from thermodynamic equation ($\Delta S_{ads} = \Delta H_{ads} - \Delta G_{ads}/T$), respectively. The $-\Delta G$ values indicate the spontaneous adsorption of inhibitor over the MS surface. The obtained adsorption isotherm plots are depicted in Figure 2. The negative sign of ΔH indicates the exothermic nature of the adsorption process, and the value of ΔH was found to be −22.65 kJ mol^{-1}, which revealed that the physisorption is effective. The ΔS_{ads} values ranged between −0.05233 and −0.04867 kJ mol^{-1} in temperature from 293 to 313 K and indicated that the adsorption is combined by means of a decrease in the disorderness of the system.[51] The evaluated thermodynamic parameter values for adsorption of *Lachancea fermentati* isolate (10^6× cfu/mL) on the mild steel surface in 0.5 M H_2SO_4 solution are given in Table 2.

The E_a values were evaluated from the plot of log(CR) against $1000/T$ (Figure 3a), and the obtained values were found to be between 68.25 and 113.20 kJ mol^{-1} (Table 3), which reveals that the physical adsorption process occurs between mild steel and *Lachancea fermentati* isolate.[51,52] Table 3 shows that when the concentration of *Lachancea fermentati* inhibitor at the transition state is increased, the values of activation parameters (E_a, ΔH, and ΔS) increase with the change in enthalpy (ΔH) values as positive and the change in entropy (ΔS) values as negative. The positive values of ΔH^* indicated the endothermic environment of the physical adsorption process, which was obtained from the slope value of the $\log(\mathrm{CR}/T)$ against $1000/T$ plot, as shown in Figure 3b.[53] The negative ΔS^* values indicated that the disorder between reactants and an activated complex was decreased. The negative ΔS^* values were evaluated the intercept values from the plot of log $RhN_A+\Delta S^*/2.303R$, which recommends the formation of biofilm over the surface of mild steel.[54]

3.3. Adsorption Isotherm Study

Interaction between the *Lachancea fermentati* isolate and MS surfaces can be well analyzed and illustrated using the adsorption theorem. Under this task, the adsorption behavior of the *Lachancea fermentati* isolate inhibitor concerning equilibrium conditions can be assessed. For this purpose, adsorption isotherm representations, such as those of Freundlich, Frumkin, Temkin, and Langmuir, can be exploited. As per the experimental results, all the isotherm representations were found to have a linear correlation (R^2 = 0.998, 0.994, 0.993, 0.991, and 0.956) and depicted the electrostatic interaction between mild steel and *Lachancea fermentati* isolate. However, among these models, the Langmuir adsorption isotherm model stood out with its very best linear fit and formation of a monolayer. This is justified by the use of *Lachancea fermentati* isolate as an inhibitor in a 0.5 M H_2SO_4 solution.[54] The data derived from the adsorption isotherm were evaluated by applying eq 8.

$$\frac{C}{\theta} = \frac{1}{K\mathrm{ads}} \times C \tag{8}$$

where θ denotes surface coverage, C denotes the concentration of *Lachancea fermentati* isolate, and K_{ads} denotes the adsorption equilibrium constant. The adsorption (Langmuir) isotherm plot for mild steel with *Lachancea fermentati* isolate in 0.5 M H_2SO_4 is given in Figure 2a,b. It is evident from the figures, which are linear with correlation coefficient (R^2 = 0.99) values, that the *Lachancea fermentati* inhibitor is adsorbed physically

https://doi.org/10.1021/acsphyschemau.3c00055
ACS Phys. Chem Au 2024, 4, 67−84

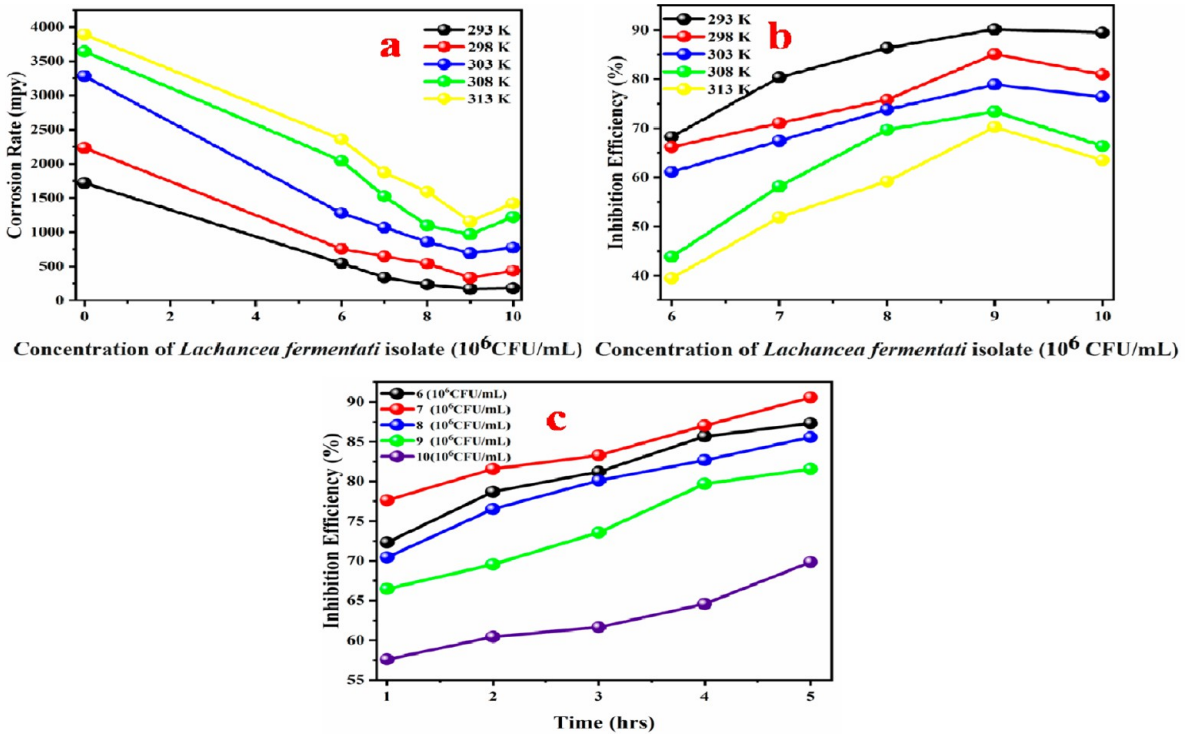

Figure 1. (a) Effect of different concentrations of *Lachancea fermentati* isolate (10^6 cfu/mL) on corrosion rate (mpy), (b) inhibition efficiency (%) at different temperatures from 293 to 313 K, and (c) effect of time (h) on inhibition efficiency (%) in different concentrations of *Lachancea fermentati* isolate in 0.5 M H_2SO_4 at 293 K.

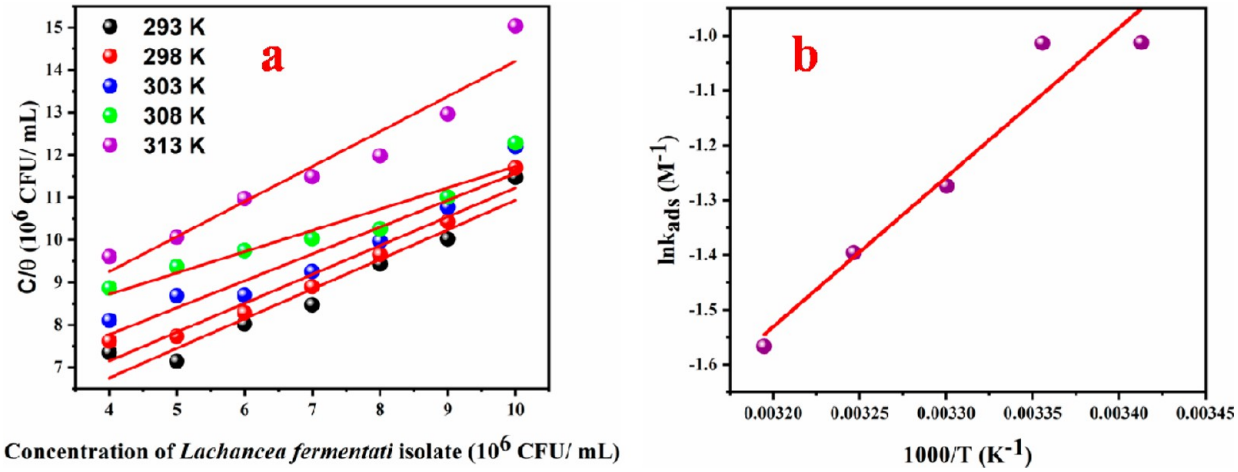

Figure 2. Adsorption isotherm: (a) Langmuir adsorption isotherm plot of different concentrations of *Lachancea fermentati* isolate (10^6 cfu/mL) in 0.5 M H_2SO_4 at 293 K and (b) adsorption isotherm plot of lnk_{ads} vs $1000/T$ (K^{-1}) for the adsorption of *Lachancea fermentati* isolate (10^6 cfu/mL) on the surface of MS at 293 K.

Table 2. Thermodynamic Parameters for Adsorption of *Lachancea fermentati* Isolate ($10^6\times$ cfu/mL) on the Mild Steel Surface in 0.5 M H_2SO_4 Solution

temperature (K)	K_{ads} 10^4 (M^{-1})	$-\Delta G_{ads}$ (kJ mol^{-1})	$-\Delta H_{ads}$ (kJ mol^{-1})	$-\Delta S_{ads}$ (kJ mol^{-1})	R^2
293	0.3632	7.3167	22.65	0.05233	0.998
298	0.3628	7.4391	22.65	0.05104	0.994
303	0.4753	8.2439	22.65	0.04754	0.993
308	0.3827	7.8252	22.65	0.48132	0.991
313	0.3114	7.4159	22.65	0.04867	0.956

on the mild steel surface under these experimental conditions.[55]

The decreased trend of corrosion rate (CR) and increased inhibition efficiency (IE %) were detected while using dissimilar concentrations of *Lachancea fermentati* isolate in 0.5 M H_2SO_4. The decreased trend of the corrosion rate indicated the formation of a protective layer (biofilm) over the mild steel surface in 0.5 M H_2SO_4. In addition, the biofilm formation on the mild steel surface provides superior surface coverage and abridges the active sites of corrosion on mild steel.[56] Furthermore, an increasing inhibition efficiency (IE %) trend was attained when the concentrations of *Lachancea fermentati* isolate in 0.5 M H_2SO_4 were increased, and the

https://doi.org/10.1021/acsphyschemau.3c00055
ACS Phys. Chem Au 2024, 4, 67−84

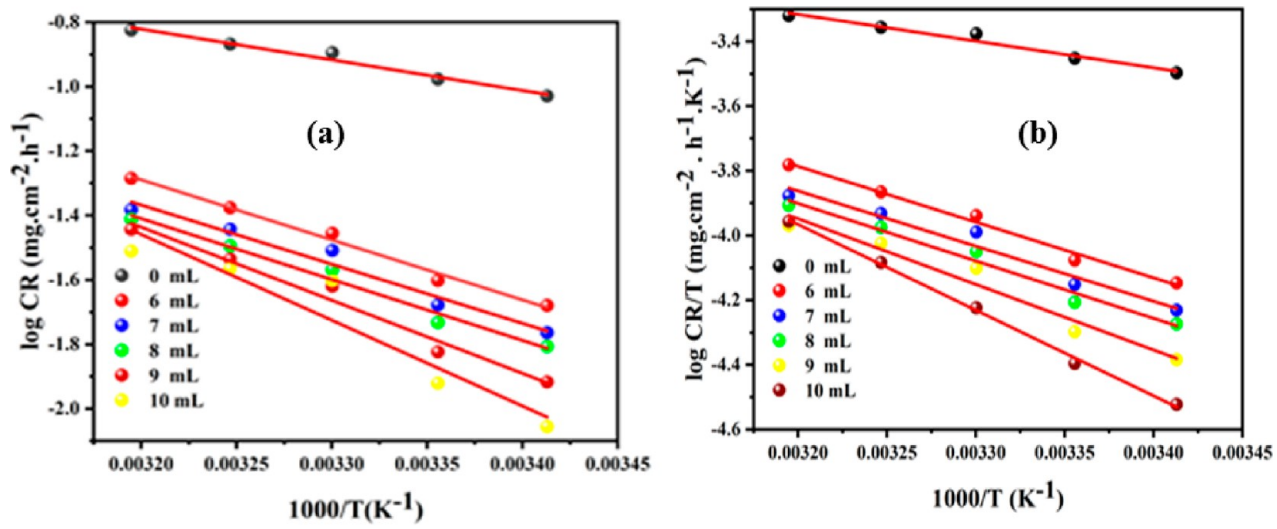

Figure 3. (a) Arrhenius plot [log(CR) vs 1000/T] and (b) Transition state plot [log(CR/T) vs 1000/T] for the adsorption of *Lachancea fermentati* isolate (10^6 cfu/mL) on the surface of MS at 293 K.

Table 3. Arrhenius Activation Parameters for Adsorption of *Lachancea fermentati* Isolate ($10^6\times$ cfu/mL) on the Mild Steel Surface in 0.5 M H_2SO_4 Solution

Lachancea fermentati isolate concentration ($10^6\times$ cfu/mL)	E_a (kJ mol^{-1})	ΔH^* (kJ mol^{-1})	$-\Delta S^*$ (kJ mol^{-1})
0	68.25	64.89	150.85
6	92.57	88.30	182.69
7	95.20	92.65	210.75
8	106.87	100.60	265.80
9	116.58	110.00	302.51
10	113.20	108.94	300.56

maximum inhibition efficiency was attained at a 9 × 10^6 cfu/mL concentration of *Lachancea fermentati* isolate. Consequently, increase of the concentration of *Lachancea fermentati* isolate over 9 × 10^6 cfu/mL showed decreased inhibition efficiency (IE %) because of molecular collision among the molecules during adsorption on the mild steel surface.[55] Thus, the 9 × 10^6 cfu/mL of *Lachancea fermentati* isolate concentration was fixed as an optimum concentration for this study.

3.4. Evaluation of Open Circuit Potential (OCP)

Under the fairest experimental setup, the fabricated working electrode was used for 30 min, which exhibited the attainment of steady-state condition. As a result, the stabilized OCP was plotted versus time, as illustrated in Figure. 4, from −100 to 1100 h. The initial OCP was found to be −469 mV in (a) 0.5 M H_2SO_4, (b) 6 mL of *Lachancea fermentati* isolate (−508 mV), (c) 7 mL of *Lachancea fermentati* isolate (−485 mV), (d) 8 mL of *Lachancea fermentati* isolate (−494 mV), (e) 9 mL of *Lachancea fermentati* isolate (−496 mV), and (f) 10 mL of *Lachancea fermentati* isolate (∼494 mV). The constant OCP was attained for almost constant (∼494 mV) for 9 × 10^6 cfu/mL for *Lachancea fermentati* isolate, and the difference between the blank and *Lachancea fermentati* isolate was found to be 39 mV at 283 K. The obtained OCP trend revealed that the potential shifts to the anodic side while adding the *Lachancea fermentati* isolate.[57] This result was ascribed to the MS degradation and also the biofilm formation as a corrosive yield on its surface. So, it is clear that with the presence of *Lachancea*

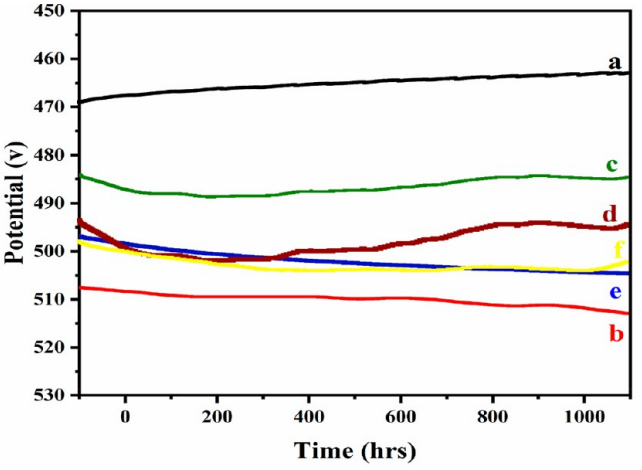

Figure 4. Open circuit potential. Potentiodynamic polarization curves for MS with and without *Lachancea fermentati* isolate (10^6 cfu/mL) at 293 K: in (a) 0.5 M H_2SO_4, (b) 6 mL of *Lachancea fermentati* isolate (−508 mV), (c) 7 mL of *Lachancea fermentati* isolate (−485 mV), (d) 8 mL of *Lachancea fermentati* isolate (−494 mV), (e) 9 mL of *Lachancea fermentati* isolate (−496 mV), and (f) 10 mL of *Lachancea fermentati* isolate (∼494 mV).

fermentati isolate, the potential shifts in the anodic direction attain rapid stability with time. This factor can well be observed by protecting film formation over the MS surface.[55]

3.5. EIS Study

Electrochemical impedance spectroscopy (EIS) data obtained from the Nyquist plot data fitted with the appropriate equivalent electrical circuit is depicted in Figure 5a−c in this electrochemical system with and without inhibitor. Here, note that these circuits yielded astounding fit outcomes. In this equivalent circuit, R_s is the solution resistance and R_{ct} is the charge transfer resistance. This equivalent circuit fitting enabled the evaluation of double-layer capacitance (C_{dl}), and the obtained data are presented in Table 4.

The electrochemical impedance spectra of MS specimens immersed without and within the *Lachancea fermentati* isolate containing 0.5 M H_2SO_4 are shown in Figure 5a. The acquired EIS spectrum exhibited an increasing trend of the R_{ct} value

https://doi.org/10.1021/acsphyschemau.3c00055
ACS Phys. Chem Au 2024, 4, 67−84

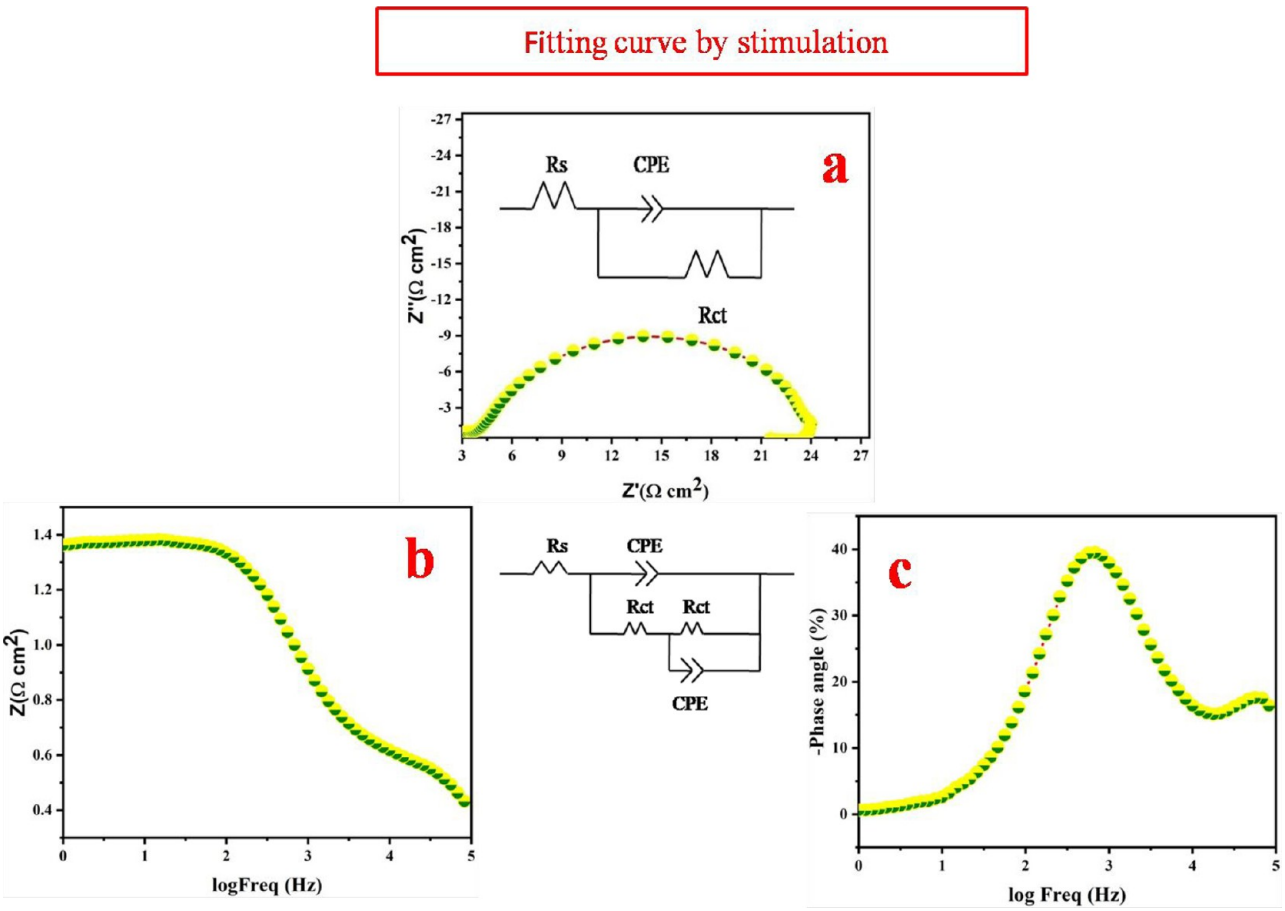

Figure 5. Stimulation of Nyquist (a) and Bode (b,c) plots with equivalent circuit of *Lachancea fermentati* isolate (10^6 cfu/mL) on the mild steel in 0.5 M H_2SO_4 solution.

Table 4. Electrochemical Impedance Parameter for the Corrosion Inhibition Process of Mild Steel in 0.5 M H_2SO_4 in the Absence and the Presence of *Lachancea fermentati* Isolate (10^6 cfu/mL)

concentration (10^6 cfu/mL)	R_S (Ω cm^{-2})	R_{ct} (Ω cm^{-2})	C_{dl} (F cm^{-2})	N	f_{max} (Hz)	IE (%)
0	3.551	20.09	0.01747	0.86	32.57	
6	7.456	43.59	3.32×10^{-4}	0.72	25.13	50.23
7	3.158	57.26	1.77×10^{-4}	0.74	22.59	63.86
8	1.866	141.31	1.95×10^{-5}	0.80	19.42	85.35
9	2.589	152.68	1.69×10^{-5}	0.85	16.26	86.45
10	1.372	147.92	1.79×10^{-5}	0.85	16.91	86.01

when *Lachancea fermentati* inhibitor concentrations were increased. This effect illustrated the best interrelationship with the data acquired from the gravimetric method. As evident from Figure. 6a, the Nyquist plot was inspected, and the CPE (constant phase element), R_{ct}, and C_{dl} values were found from eqs 9−11.

$$Z_{CPE} = (Y_0)^{-1}[(j\omega)]^{-1} \tag{9}$$

$$Y_{CPE} = Y_0(j\omega)^n \tag{10}$$

where Y_0 denotes the CPE constant; n denotes the exponent of the CPE for evaluating phase shift, which is used to calculate the surface ruggedness ($0 < n < 1$); and ω denotes angular frequency. Similarly, n = 0, 0.5, 1, and −1, respectively.

$$C_{dl} = \frac{1}{2\pi f_{max} R_{ct}} \times 100 \tag{11}$$

where R_{ct} is the charge transfer resistance, C_{dl} is the double-layer capacitance, and f_{max} represents the impedance frequency. EIS parameters, such as solution resistance (R_s), charge transfer resistance (R_{ct}), and double-layer capacitance (C_{dl}) values, were evaluated from the equivalent circuit fitting measured for frequencies from 100 kHz to 10 MHz. The EIS spectrum of MS without and with *Lachancea fermentati* isolate in 0.5 M H_2SO_4 and the obtained EIS spectra revealed that the charge transfer resistance (R_{ct}) increased as the *Lachancea fermentati* isolate concentrations increased, which resulted in good correlation with the data obtained from the weight loss method. The C_{dl} values were found to decrease from 1.74×10^2 to 1.79×10^{-5}, which supports the charge transfer process that occurs between mild steel and *Lachancea fermentati* isolate. However, the R_{ct} values increased from 20.09 Ω cm^2 to 152.68 Ω cm^2, which indicated that the *Lachancea fermentati* isolate formed a protective layer over the mild steel surface while increasing the concentration of *Lachancea fermentati* isolate.[56]

https://doi.org/10.1021/acsphyschemau.3c00055
ACS Phys. Chem Au 2024, 4, 67−84

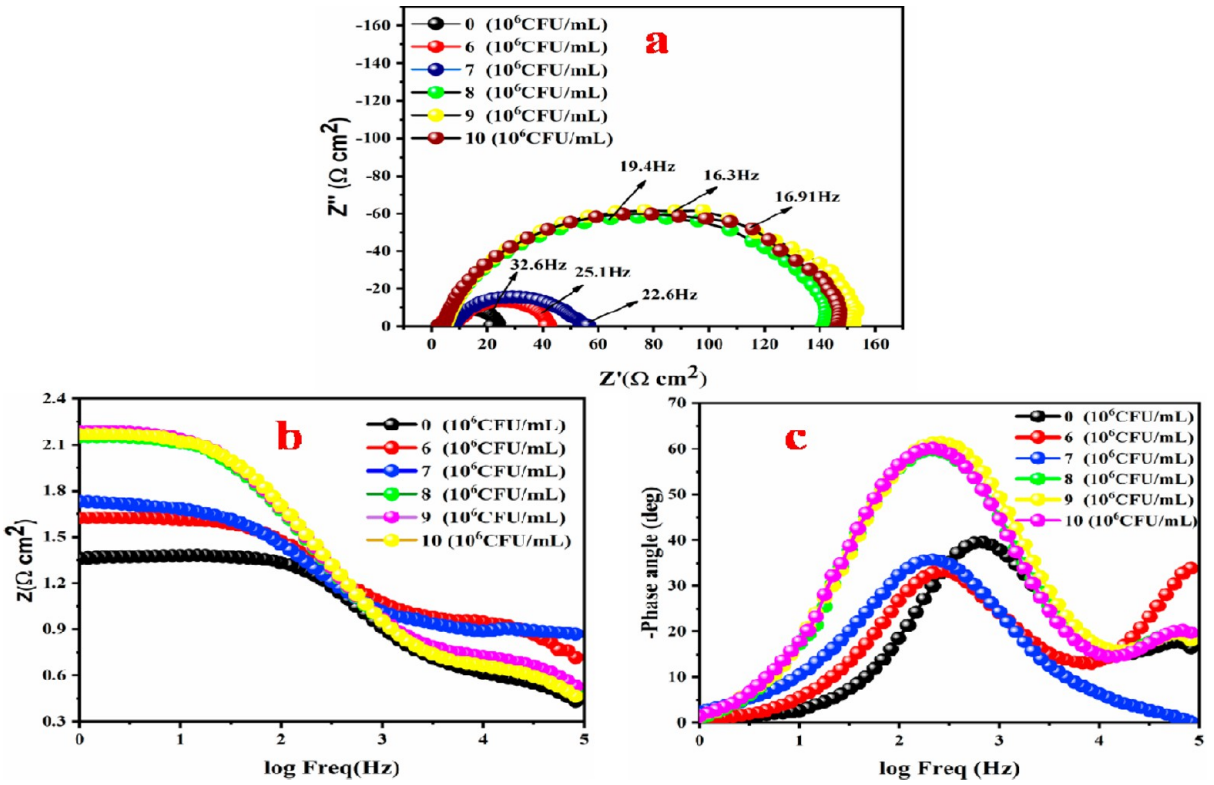

Figure 6. (a) Nyquist, (b) Bode total impedance, and (c) phase angle plots against frequency (Hz) for MS immersed in 0.5 M H_2SO_4 in the presence and absence of *Lachancea fermentati* isolate (10^6 cfu/mL) at 293 K.

Similarly, there had been an appreciable improvement in inhibition efficiency due to increased R_{ct} values, along with inhibitor concentration. The increased R_{ct} values were found to be the maximum IE of 90% at the optimal *Lachancea fermentati* isolate concentration (i.e., 9 × 10^6 cfu/mL). The phase angle and Bode diagrams clearly showed that the increased phase angle values were caused by varying *Lachancea fermentati* isolate concentrations in 0.5 M H_2SO_4. This is conceded because of biofilm formation as a protective layer by *Lachancea fermentati inhibitor* on mild steel and the decrease in the roughness of the metal exterior.[49,58,59]

3.6. Potentiodynamic Polarization (PDP) Study

The PDP study was done to examine the inhibitive nature and potential of the *Lachancea fermentati* isolate on the MS surface. Subsequently, the study investigated MS in 0.5 M H_2SO_4 at various concentrations of *Lachancea fermentati* isolate and the absence of *Lachancea fermentati* isolate at room temperature. PDP curves derived from this analysis are depicted in Figure. 7. The Tafel polarization parameters, such as corrosion potential (E_{corr}), corrosion current density (i_{corr}) (mV vs SCE), cathodic and anodic Tafel slopes (β_c and β_a), and inhibition efficiency (IE %) values, were evaluated from polarization curves, and their corresponding values and IE % are presented in Table 5. The obtained polarization curves for a given potential value indicate that the decrease of i_{corr} value and corrosion rate with the addition of *Lachancea fermentati* isolate and improves the surface coverage (θ) on the MS (i.e., working electrode) surface by means of adsorption method.[60] From Table 5, it was observed clearly that the i_{corr} values decreased from 1689 to 169.2 μA cm^{-2}, and the yield of inhibition efficiency ranged from 64.89% to 90.00% when the concentration of *Lachancea fermentati* inhibitor was increased. In addition, the E_{corr} values

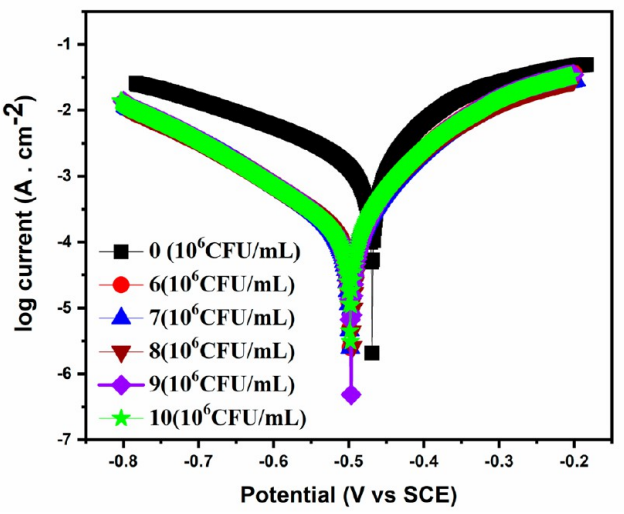

Figure 7. Tafel plot for MS immersed in 0.5 M H_2SO_4 in the presence and absence of *Lachancea fermentati* isolate (10^6 cfu/mL) at 293 K.

were shifted to some extent (56 mV) toward anodic side, thereby indicating that the *Lachancea fermentati* isolate behaves as a mixed type of inhibitor but leads the anodic process because of a slow down in hydrogen evolution. The maximum IE % of *Lachancea fermentati* isolate for Tafel polarization curves was calculated to be 90.0% at optimized concentration (9 × 10^6 cfu/mL).

These data revealed that the *Lachancea fermentati* isolate acted as a mixed corrosion inhibition type reaction, but the predominant reaction was cathodic controlled. Thus, it can be presumed that the mechanism of adsorption of *Lachancea*

https://doi.org/10.1021/acsphyschemau.3c00055
ACS Phys. Chem Au 2024, 4, 67−84

Table 5. Tafel Plots of Mild Steel Immersed in 0.5 M H_2SO_4 with and without *Lachancea fermentati* Isolate (10^6 cfu/mL)

concentration (10^6 cfu/mL)	$-E_{corr}$ (mV)	$-i_{corr}$ (μA cm^{-2})	$-\beta_c$ (mV dec^{-2})	$-\beta_a$ (mV dec^{-2})	R_p (Ω)	IE (%)
0	454	1689.0	189	122	19	
6	510	593.0	156	116	31	64.89
7	484	389.7	131	89	115	76.92
8	494	175.0	136	90	135	89.63
9	497	169.2	134	92	141	90.00
10	498	179.7	135	91	132	89.36

fermentati isolates on the MS surface was influenced by anodic dissolution with cathodic hydrogen evolution. Here, it was observed that the presence of the *Lachancea fermentati* isolate could yield higher R_p (polarization resistance) values than the uninhibited solution. Also, there was a definite formation of the biofilm when *Lachancea fermentati* isolate was added to the MS surface. Moreover, the electrochemical (potentiodynamic polarization and EIS) techniques exhibited the highest IE % (90%) under an optimal concentration of 9 × 10^6 cfu/mL, which was in best agreement with each other. To prove the inhibition efficiency of *Lachancea fermentati* isolate, it was compared with a microbial inhibitor that was extracted by methanol and by inducing *Bacillus megaterium* to *Artemisia pallens*.[43] The comparative analysis showed that the maximum IE % (83%) was attained at 25 ppm concentration of microbial inhibitor concentration, and the highest IE % (87%) was obtained for a 10^4 cfu/mL concentration of formed glycolipid biosurfactant intermediate−microbial inhibitor intermediate, whereas the present work exhibited the highest IE % (90%) for the 9 × 10^6 cfu/mL of *Lachancea fermentati* concentration. Thus, the corrosion inhibition potential of *Lachancea fermentati* isolate is comparable with other microbial inhibitors.[61]

3.7. UV−visible Spectral Study

In this study, an iron complex was formed through the interaction of iron species from MS with binding sites of the *Lachancea fermentati* isolate, which could be easily examined by a UV−visible spectrophotometer. The UV−vis spectrum of *Lachancea fermentati* isolate is shown in Figure. 8a, which exhibits a peak absorption range between 243 and 290 nm. This elevated range was made possible because of the occurrence of a transition in the inhibitor due to n−σ*. Similarly, Figure. 8b showed the UV−vis spectrum of 9 × 10^6 cfu/mL of *Lachancea fermentati* isolate with MS specimen in 0.5 M H_2SO_4 for 2 h. The spectrum exhibited electronic transitions of the inhibitor (π−π* and n−π*) and its transition peaks at 249 and 306 nm, respectively. This easily leads to the corresponding peak of transitions observed with polysaccharides, thereby indicating carboxyl functional groups exist in the *Lachancea fermentati* isolate.[55] As per the UV−vis absorption spectrum of the *Lachancea fermentati* isolate with MS, there was an increase in absorbance and a shift in the wavelength compared with the *Lachancea fermentati* isolate. The result indicated that the increase in intensity and shifting of absorption wavelength in the UV−vis spectrum was due to the formation of a complex between *Lachancea fermentati* isolate and MS.[54,56]

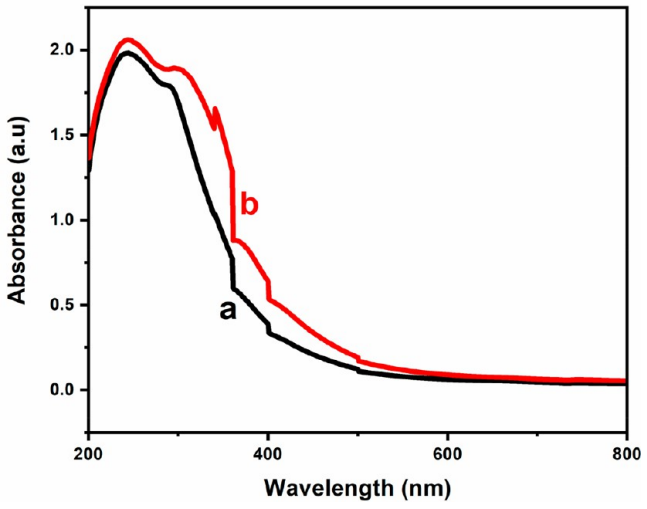

Figure 8. UV−visible spectrum of solution containing 0.5 M H_2SO_4 before (a) and after (b) the MS immersed in 9 × 10^6 cfu/mL of *Lachancea fermentati* isolate.

3.8. FT-IR Spectral Study

Lachancea fermentati inhibitor and a scratched sample of *Lachancea fermentati* inhibited on the mild steel surface in 0.5 M H_2SO_4 are analyzed by the FT-IR technique. The experimental results are illustrated in Figure 9a,b. As per the analysis, the FT-IR spectra of *Lachancea fermentati* and a scratched sample of *Lachancea fermentati* deposited on the mild steel surface exposed similar peaks. From Figure 9a, the wide FT-IR peaks could be noticed at 3491 and 3460 cm^{-1}, which correspond to O−H (hydroxyl group) stretching, while the stretching frequencies at 2050, 1628, and 1035 cm^{-1} correspond to C═C, C═O, and C−O−C stretching

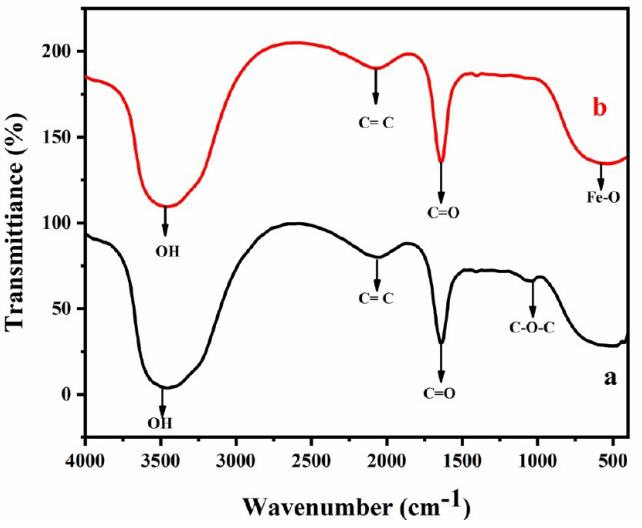

Figure 9. FT-IR spectrum of (a) 9 × 10^6 cfu/mL of *Lachancea fermentati* isolate and (b) *Lachancea fermentati* isolate scratched from MS surface after immersion in 0.5 M H_2SO_4 with 9 × 10^6 cfu/mL of *Lachancea fermentati* isolate.

https://doi.org/10.1021/acsphyschemau.3c00055
ACS Phys. Chem Au 2024, 4, 67−84

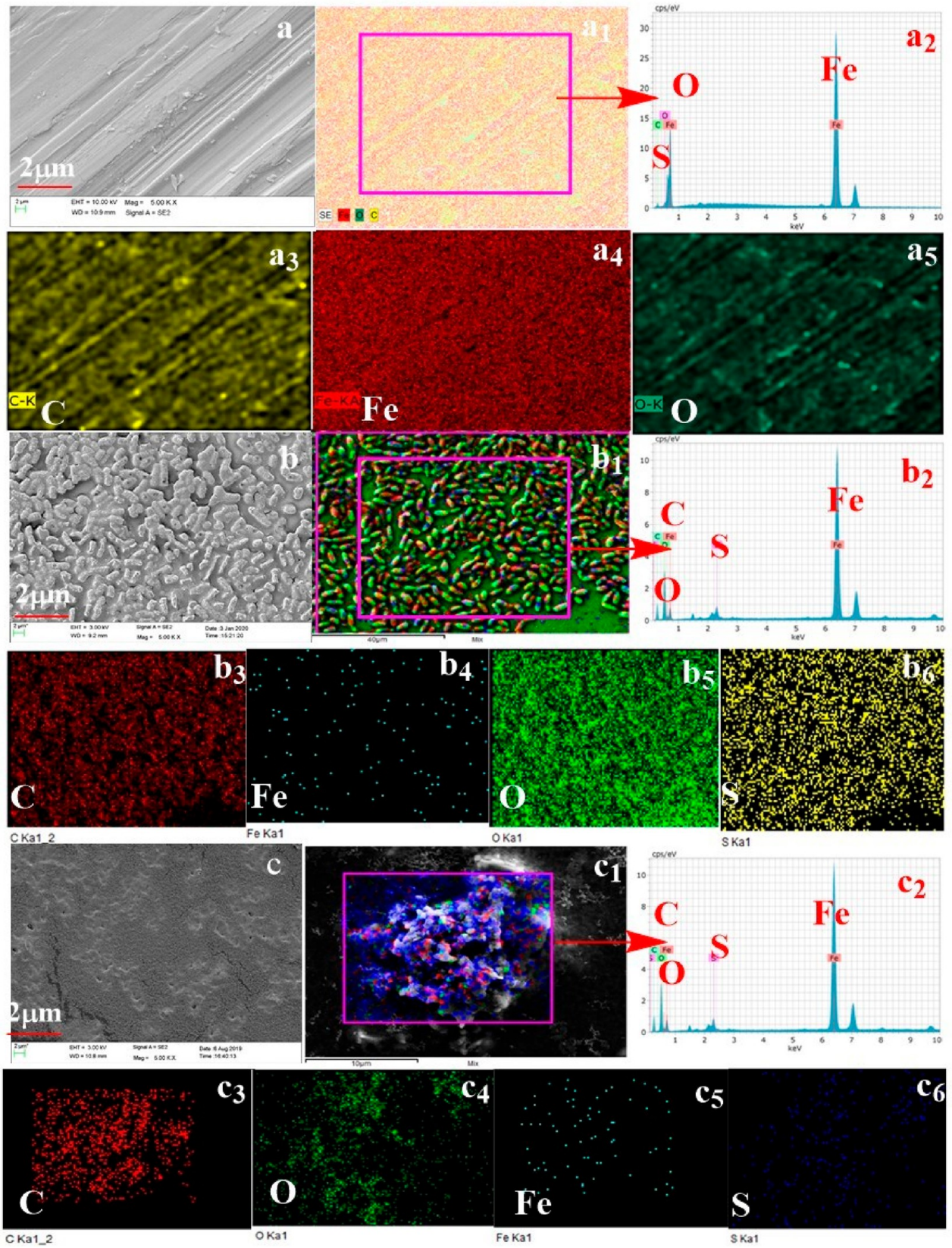

Figure 10. (a) FE-SEM of polished MS; (a_1) overall mapping elements on the same spot corresponding to (a_2) EDXS micrograph and (a_3) carbon, (a_4) oxygen, and (a_5) Fe mapping analysis of polished MS. (b) FE-SEM of corroded MS; (b_1) overall mapping elements on the same spot corresponding to (b_2) EDXS micrograph and (b_3) carbon, (b_4) oxygen, (b_5) Fe, and (b_6) sulfur mapping analysis of MS immersed in 0.5 M H_2SO_4. (c) FE-SEM of mild steel; (c_1) overall mapping elements on the same spot corresponding to (c_2) EDXS micrograph and (c_3) carbon, (c_4) oxygen, (c_5) Fe, and (c_6) sulfur mapping analysis of mild steel immersed in 0.5 M H_2SO_4 containing (9×10^6 cfu/mL) *Lachancea fermentati* isolate.

https://doi.org/10.1021/acsphyschemau.3c00055
ACS Phys. Chem Au 2024, 4, 67−84

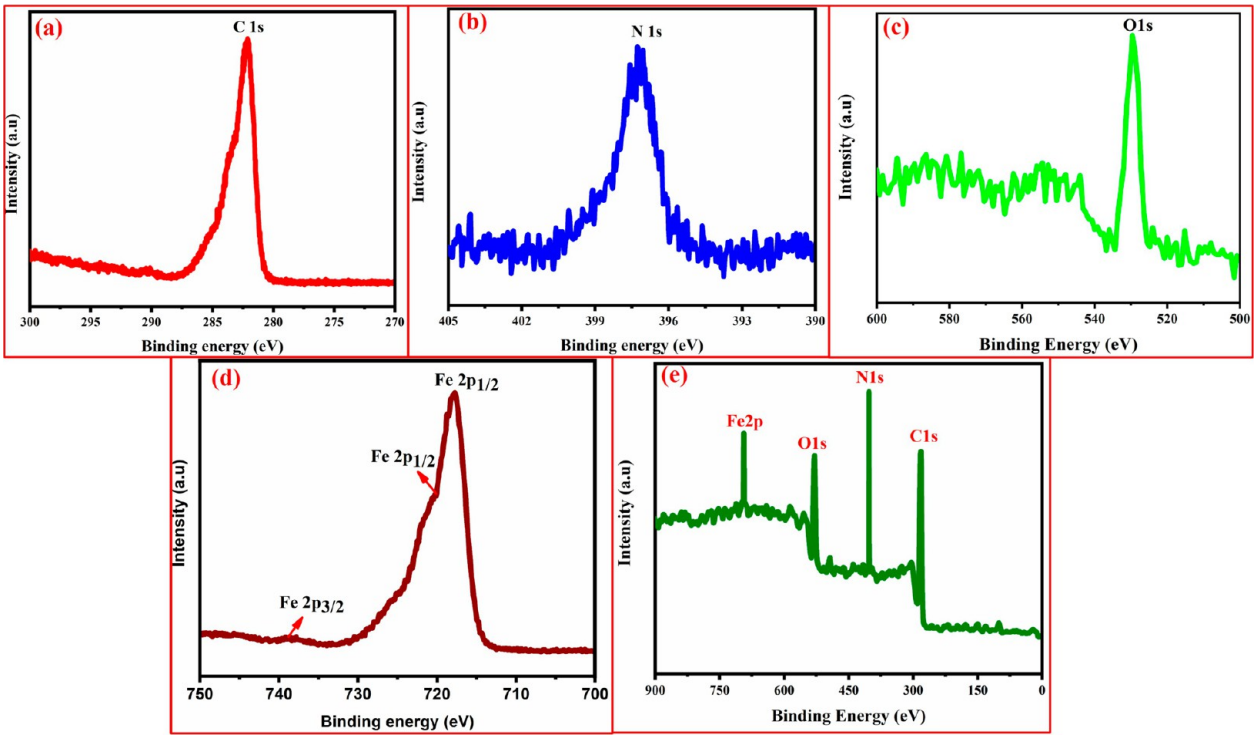

Figure 11. XPS spectra of (a) C 1s, (b) N 1s, (c) O 1s, and (d) Fe 2p3/2. (e) XPS survey scan spectrum of *Lachancea fermentati* isolate biofilm adhesion on MS surface at an exposure time of 3 h in 0.5 M H_2SO_4 and 9 × 10^6 cfu/mL of *Lachancea fermentati* isolate.

frequencies for polysaccharide.[62] Further, when the FT-IR spectrum was exposed to a *Lachancea fermentati* isolate scratched sample, as observed in Figure 9b, there were intense peaks at 2068 and 1628 cm^{-1} indicating the presence of C═C and C═O functionalities in *Lachancea fermentati* isolate adsorption. However, the FT-IR spectrum of *Lachancea fermentati* inhibited on the MS surface displayed an extra FT-IR peak at 578 cm^{-1} for the iron species behind adsorption. Furthermore, it can be attributed to the integration of *Lachancea fermentati* isolate on MS surfaces.[63,64]

3.9. FE-SEM, EDXS, and Mapping Study

The structural insights and surface morphology of MS specimens with and without *Lachancea fermentati* isolates were analyzed using FE-SEM, EDXS, and mapping analysis, and the results are illustrated in Figure 10. Figure 10a−a_5 displays the FE-SEM images of MS specimens in 0.5 M H_2SO_4 and after immersion into *Lachancea fermentati* isolates in 0.5 M H_2SO_4 medium. The SEM images showed a soft and glittering surface of MS because of the existence of a *Lachancea fermentati* isolate. The EDX technique enabled the investigation of the percentage composition of elements present in the scratched sample of *Lachancea fermentati* isolate with an MS specimen, and the obtained results are depicted in Figure 10b−b_6: (b_1) exposes the element presence by mapping; (b_2) depicts the exposure of EDXS, while other figures displays the elements' existence; and (b_3) carbon, (b_4) iron, (b_5) oxygen, and (b_6) sulfur for mild steel specimens are engrossed in 0.5 M H_2SO_4 medium. Concrete analyses of this experimental study duly revealed the biofilm formation due to the existence of *Lachancea fermentati* isolate (9 × 10^6 cfu/mL) over the mild steel surface. Figure. 10c shows the reduction of the straight attack of 0.5 M H_2SO_4 and, also, the abridged corrosion rapidity of the MS surface. Figure 10 panel (c_1) exposes the element presence by mapping; (c_2) depicts the exposure of EDXS, while other figures displayed the elements' existence; and (c_3) carbon, (c_4) iron, (c_5) oxygen, and (c_6) sulfur for mild steel specimens are engrossed in 0.5 M H_2SO_4 medium. The experimental data reveals that the MS specimen was protected by a thin layer (biofilm formation) on its surface due to electrostatic attraction between the MS and *Lachancea fermentati* isolate in H_2SO_4 medium.[65,66]

3.10. XPS Study

The formation of biofilm on the surface of MS was investigated by X-ray photoelectron spectroscopy (XPS). The XPS spectra were analyzed between the ranging of binding energies from 0 to 900 eV, and the obtained spectra are depicted in Figure 11. The XPS spectra of *Lachancea fermentati* isolate biofilm formation on the MS surface provide evidence about the elements and their chemical states. The XPS spectrum of *Lachancea fermentati* isolate biofilm adhesion on MS surface revealed the presence of carbon (C), iron (Fe), oxygen (O), and nitrogen (N) elements (Figure 11e). Figure 11a shows the binding energy value at 281.95 eV for the C 1s state because of the presence of the C−C bond in *Lachancea fermentati* isolate.[61,67,68] Figure 11b exhibits the binding energy value at 398.56 eV for the N 1s state because of the −CO−NH (imide) bond.[55,56,61] Figure 11c exhibits the binding energy (eV) value at 526.00 eV for the O 1s chemical state. Figure 11d shows the binding energy values at 715.03 eV for Fe−OOH/Fe_2O_3, at 718.80 eV for Fe−OOH, and at 735.62 eV for Fe^{3+} peaks for iron atoms.[69,70] The elements, such as carbon (C), iron (Fe), oxygen (O), and nitrogen (N), were confirmed, and the aforementioned elements were involved for the formation of biofilm (protective layer) over the surface of MS via electrostatic interactions.

https://doi.org/10.1021/acsphyschemau.3c00055
ACS Phys. Chem Au 2024, 4, 67−84

3.11. AFM Study

AFM analysis was used to study the control rate of the *Lachancea fermentati* isolate over the MS surface and the protective layer formation at the metal/solution interface. AFM image analysis gave the R_a, R_q, and $P-V$ values, which are listed in Table 6. From the table, it is evident that the average roughness (R_a) values of the MS surface in the presence of the *Lachancea fermentati* isolate are lower than those in the absence of the *Lachancea fermentati* isolate. In addition, a decrease in average roughness values was observed after addition of the *Lachancea fermentati* inhibitor. Furthermore, the protection of the MS specimen by biofilm had been secreted from *Lachancea fermentati* inhibitor. Figure 12 demonstrates the comparative analysis of the 2D- and 3D-dimensional AFM images of the MS specimen in a 0.5 M H_2SO_4 solution in the absence and the presence of *Lachancea fermentati* inhibitors. The AFM images (Figure 12 a,a_1) for a polished MS surface provide the R_a value (8.25 nm), R_q value (10.18 nm), and $P-V$ value (42.18 nm). Figure 12b,b_1 displays the corroded MS surface images with sharpened, shaped particles on its surface and provides the R_a value (83.55 nm), R_q value (98.73 nm), and $P-V$ value (408.05 nm). The AFM results indicated that the coarse surface of the MS specimen was acquired by 0.5 M H_2SO_4 attack, whereas the adsorbed film covering the MS surface was obtained after adding 9×10^6 cfu/mL of *Lachancea fermentati* isolate into 0.5 M H_2SO_4 solution, as depicted in Figure. 12c,c_1. It exhibited a smooth surface texture, which evidenced that the biofilm formed over the MS surface and that the corrosion rate of the MS was found to be reduced. Calculated values of R_a, R_q, and $P-V$ for MS specimens were found to be 9.8302, 13.62, and 87.78 nm, respectively. The obtained data authenticated the biofilm formation as a protective layer on the MS surface by *Lachancea fermentati* inhibitors and enabled smooth MS surfaces. Moreover, the obtained AFM results in this study followed the literature's AFM results.[71,72]

Table 6. AFM of MS Immersed in 0.5 M H_2SO_4 and *Lachancea fermentati* Isolate

samples	R_q (nm)	R_a (nm)	$R_{(P-V)}$ (nm)
Polished MS	10.183	8.249	42.175
MS in 0.5 M H_2SO_4	98.732	83.553	408.05
MS in 0.5 M H_2SO_4 + *Lachancea fermentati* isolate	13.616	9.8302	87.78

4. DFT STUDY

Quantum chemical calculations enable us to determine the donor−acceptor relations between the FMOS (frontier molecular orbitals) of the inhibitor and the MS surface. This quantum chemical calculation involved the electronic distribution in HOMO−LUMO levels, electron density, and MESP (molecular electrostatic potential) and CESP (contour electrostatic potential). contour maps by using the density functional theory study. The calculated parameters are presented in Table 6. Geometrical optimization, distribution of electron density at HOMO−LUMO levels, and MESP surface structures of

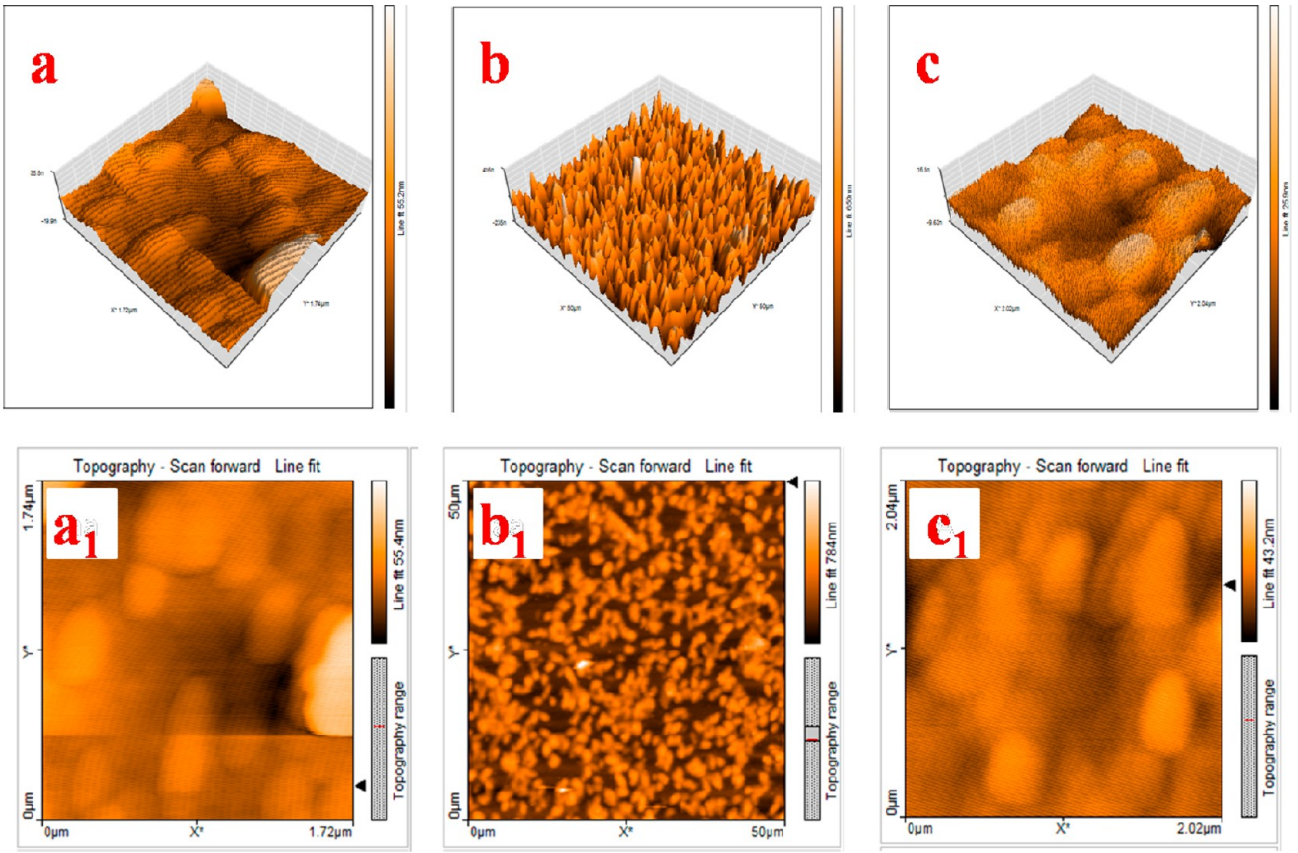

Figure 12. AFM images of (a,a_1) polished MS surface, (b,b_1) MS immersed in 0.5 M H_2SO_4, and (c,c_1) MS immersed in 0.5 M H_2SO_4 containing 9×10^6 cfu/mL of *Lachancea fermentati* isolate.

https://doi.org/10.1021/acsphyschemau.3c00055
ACS Phys. Chem Au 2024, 4, 67−84

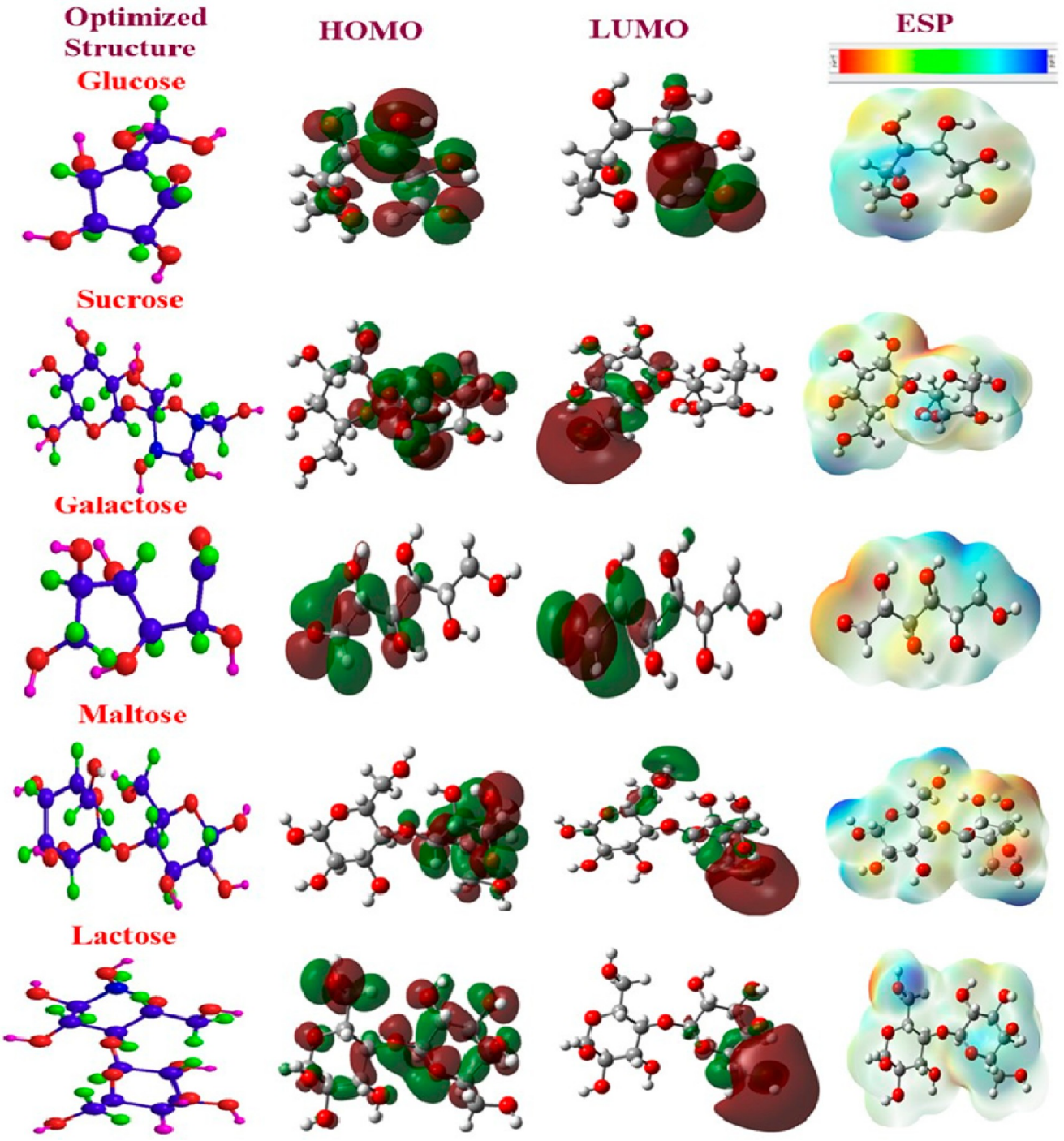

Figure 13. Optimized structures of HOMO an LUMO with ESP for *Lachancea fermentati* isolate.

Lachancea fermentati are shown in Figures 13 and 14. The MESP images from the figure show that the reactive sites of monosaccharides possess O atoms, OH groups, and aromatic double bonds, in that order. The best positive area for the *Lachancea fermentati* isolate molecule is represented by the blue zone in the figures. Similarly, the yellow zone represents the atoms having realistic electronegativity, while the red zone refers to the high electronegativity ring. Here, it is better to record that the electronegativity ring is highly recommended for electrophilic attacks.

Figure 13 depicts the comparative merits of galactose molecules about electron-rich sites compared with glucose, sucrose, maltose, and lactose molecules. This superiority indicates the effective transfer of electrons by galactose to its electron pairs, by which a bond with iron in MS is formed. Thus, galactose proves its worth by having more potential than glucose and maltose. The results prove the possibility of offering the electron pairs of the molecules as follows: galactose > glucose > maltose > lactose > sucrose. Next, the two- and three-dimensional plots of the protonated and neutral structures of the galactose molecule were observed for examination. The results displayed the distribution of electron densities of the LUMO and HOMO in the functional groups and aromatic double bonds as equal. Structurally, the

https://doi.org/10.1021/acsphyschemau.3c00055
ACS Phys. Chem Au 2024, 4, 67−84

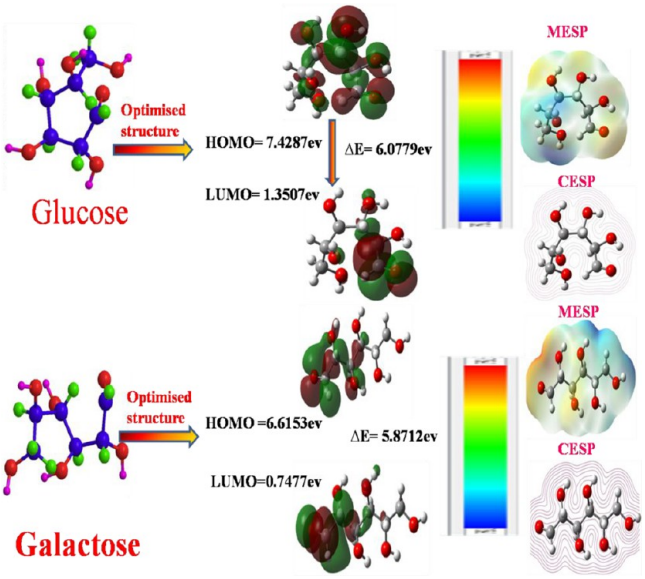

Figure 14. Short explanation of optimized structures of HOMO and LUMO with ESP for *Lachancea fermentati* isolate.

Lachancea fermentati isolate mostly envelopes the glucose and galactose molecules because of inhibition effects. Consequently, a density functional theory study has been carried out by considering galactose and glucose molecules. Meanwhile, the DFT study can give a corresponding assessment of the optimized chemical structure, energy gap (ΔE) between E_{HOMO} and E_{LUMO} (energy gap = $E_{HOMO} - E_{LUMO}$), and the number of transferred electrons (ΔN), respectively. All observed results are shown in Figure 14, while the evaluated DFT data are presented in Table 7.

Comparatively, for galactose (ΔE = 5.8712 eV), a much lower value could be observed than for glucose (ΔE = 6.0779 eV), which justifies the enhanced potential of biofilm formation on the mild steel surface. The low value (ΔN < 3.6) was calculated, which supports the transfer of electrons from galactose to form a metal−ligand complex with a mild steel surface due to electrostatic interaction. The highly polarizable galactose molecules almost reached contact with the MS surface while covering a larger surface area to provide better corrosion inhibitor performances. The data derived from CEPS and MESP maps illustrated the existence of electron-rich oxygen atoms from carbonyl groups, hydroxyl groups, and aromatic-ring-conjugated double bonds. These bonds are involved in biofilm formation over the mild steel surface under experimental conditions.[73−75]

5. MECHANISM

All of the experimental results obtained in this study affirmed that the *Lachancea fermentati* isolate acted as a potential inhibitor via biofilm formation over the mild steel surface in an acid medium. Weight loss measurements revealed the decreased inhibition efficiency (%) at high temperatures, which supported the occurrence of the physisorption. The FT-IR results acknowledged the presence of polysaccharides, as well as galactose, in the *Lachancea fermentati* isolates. It paves the way for metal−ligand complex formation because of electrostatic interaction. The stretching frequency of functionalities present in the *Lachancea fermentati* isolate was responsible for biofilm formation on the mild steel surface because of the existence of monosaccharide constituents in the *Lachancea fermentati* isolate. By this phenomenon, galactose was observed to act as a Lewis base, and it was further noticed that galactose donated two nonbonded electrons from −OH groups to unoccupied Fe d orbitals in mild steel. Under the *Lachancea fermentati* process, galactose mostly acted as a blocking source in the existing active sites on the mild steel surface to stop more corrosion via biofilm formation. During this stage, the energy difference of the HOMO−LUMO (ΔE) value was estimated to be much less, thereby favoring the physisorption process between *Lachancea fermentati* isolate and mild steel. The occurrence of monolayer adsorption type (i.e., physisorption) between the mild steel surface and *Lachancea fermentati* inhibitor in 0.5 M H_2SO_4 was verified by the Langmuir adsorption isotherm data.[55,56,61] On the basis of the experimental and theoretical results, a suitable metal inhibitor electrostatic interaction mechanism in 0.5 M H_2SO_4 is presented in Scheme 2.

Scheme 2. Suitable Corrosion Inhibition Mechanism for MS in the Presence of *Lachancea fermentati* Inhibitor in 0.5 M H_2SO_4

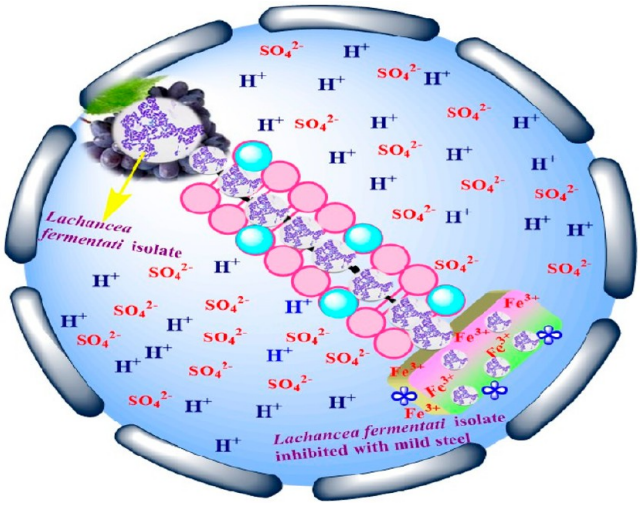

Table 7. Quantum Chemical Parameters for Pytochemicals Present in *Lachancea fermentati* Isolate

phytochemicals	E_{HOMO} (eV)	E_{LUMO} (eV)	ΔE (eV)	X	H	σ	IE	EA	ΔN_{110}
glucose	7.4287	1.3507	6.0779	4.3897	3.0389	0.3291	−7.4287	−1.3507	0.0309
sucrose	6.9574	0.0400	6.9574	3.5187	3.4787	0.2875	−6.9574	−0.0400	0.0814
galactose	6.6153	0.7477	5.8712	3.6801	2.9353	0.3407	−6.6153	−0.7448	0.0768
maltose	6.5245	0.1812	6.5245	3.4435	3.2622	0.3065	−6.7057	−0.1812	0.0863
lactose	6.9634	0.0914	6.8719	3.5274	3.4359	0.2910	−6.9634	−0.0914	0.0831

https://doi.org/10.1021/acsphyschemau.3c00055
ACS Phys. Chem Au 2024, 4, 67−84

6. CONCLUSION

Lachancea fermentati isolate was successfully extracted from rotten grapefruits, and its potential for corrosion inhibition in mild steel was examined in 0.5 M H_2SO_4. All characterization results match well with the structural insights of the corrosion inhibitor used in this study. The highest inhibition efficiency (IE = 90%) was calculated in the weight loss study, and results revealed that by increasing the concentration of *Lachancea fermentati* isolate, the inhibition efficiency increased. The physisorption reaction was found to be suitable between the *Lachancea fermentati* inhibitor and mild steel and followed the Langmuir adsorption isotherm kinetics. Tafel polarization study data divulged that the mixed type of corrosion reaction (anodic and cathodic) occurs predominantly because of the presence of reductive functionalities in *Lachancea fermentati* isolate. The EIS study confirmed that the R_{ct} values were enhanced while increasing the *Lachancea fermentati* inhibitor concentration and also supported the biofilm formation over a mild steel surface. The biofilm formation on the surface of mild steel was successfully analyzed by FT-IR spectroscopy for confirmation of the functional groups present in the *Lachancea fermentati* isolate. Furthermore, the DFT study afforded the structural information on the *Lachancea fermentati* isolate that was in good conformity with the experimental results. The energy difference of the HOMO−LUMO (ΔE) value was estimated to be very small, thereby favoring the physisorption process between *Lachancea fermentati* isolate and mild steel because of electrostatic interaction via formation of a metal−inhibitor complex. The formation of biofilm was confirmed by surface morphological analysis, and a suitable inhibition mechanism of mild steel corrosion against *Lachancea fermentati* isolate was explained.

■ ASSOCIATED CONTENT

Supporting Information

The Supporting Information is available free of charge at https://pubs.acs.org/doi/10.1021/acsphyschemau.3c00055.

(i) Phylogenetic tree of *Lachancea* sp. isolate strain G2 (MH476356.1) constructed using the neighbor-joining method with the aid of MEGA 6.0 program, (ii) plate 1 isolation of yeast from grape fruit by spread plate method, and (iii) identification by DNA sequencing (PDF)

■ AUTHOR INFORMATION

Corresponding Authors

Durvas Seshian Bhuvaneshwari − *Department of Chemistry, Thiagarajar College, Madurai 625009 Tamil Nadu, India*; Email: dsbhuvaneshwari@gmil.com

Periyakaruppan Karuppasamy − *Department of Chemistry, Dayananda Sagar College of Engineering, Bangalore 560078 Karnataka, India*; orcid.org/0000-0003-1461-9827; Email: periyakaruppankaruppasamy@gmail.com

H C Ananda Murthy − *Department of Applied Chemistry, School of Applied Natural Science, Adama Science and Technology University, 1888 Adama, Ethiopia; Department of Prosthodontics, Saveetha Dental College & Hospital, Saveetha Institute of Medical and Technical Science (SIMATS), Saveetha University, Chennai 600077 Tamil Nadu, India*; orcid.org/0000-0002-2361-086X; Email: anandkps350@gmail.com

Authors

Baluchamy Tamilselvi − *Department of Chemistry, Thiagarajar College, Madurai 625009 Tamil Nadu, India; Department of Chemistry, K.L.N. College of Engineering, Pottapalaiyam 630612 Tamil Nadu, India*

Sethuramasamy Padmavathy − *Department of Microbiology and Biotechnology, Thiagarajar College, Madurai 625009 Tamil Nadu, India*

Santhosh Nikhil − *School of Chemistry, Madurai Kamaraj University, Madurai 625009 Tamil Nadu, India*

Surendra Boppanahalli Siddegowda − *Department of Chemistry, Dayananda Sagar College of Engineering, Bangalore 560078 Karnataka, India*

Complete contact information is available at: https://pubs.acs.org/10.1021/acsphyschemau.3c00055

Author Contributions

CRediT: **Baluchamy Tamilselvi** data curation, formal analysis, investigation; **Durvas Seshian Bhuvaneshwari** conceptualization, supervision; **Periyakaruppan Karuppasamy** methodology, writing-original draft; **Sethuramasamy Padmavathy** resources, software; **Santhosh Nikhil** resources, software; **Surendra Boppanahalli Siddegowda** writing-review & editing; **H C Ananda Murthy** writing-review & editing.

Notes

The authors declare no competing financial interest.

■ ACKNOWLEDGMENTS

The author thanks the management, Principal, and Head of the Postgraduate and Research Department of Chemistry, Thiagarajar College, for providing laboratory facilities to carry out the present work.

■ REFERENCES

(1) Fiori-Bimbi, M. V.; Alvarez, P. E.; Vaca, H.; Gervasi, C. A. Corrosion inhibition of mild steel in HCl solution by Pectin. *Corros. Sci.* **2015**, *92*, 192−199.

(2) Alaneme, K. K.; Olusegun, S. J.; Adelowo, O. T. Corrosion inhibition and adsorption mechanism studies of Hunteria umbellate seed husk extracts on mild steel immersed in acidic solutions. *Alex. Eng. J.* **2016**, *55* (1), 673−681.

(3) Singh, D. K.; Kumar, S.; Udayabhanu, G.; John, R. P. 4(N,N-dimethylamino) benzaldehyde nicotinic hydrazone as corrosion inhibitor for mild steel in 1M HCl solution: An experimental and theoretical study. *J. Mol. Liquid.* **2016**, *216*, 738−746.

(4) Koch, G. H.; Brongers, M. P. H.; Thompson, N. G.; Virmani, Y. P.; Payer, J. H. Corrosion costs and preventive strategies in the United States. *Report FHWA-RD-01−156*, **2003**.

(5) Zuo, R. Biofilms:strategies for metal corrosion inhibition employing microorganism. *Appl. Microbiol. Biotechnol.* **2007**, *76* (6), 1245−1253.

(6) Muthamma, K.; Kumari, P.; Lavanya, M.; Rao, S. A. Corrosion Inhibition of Inhibition of Mild Steel in Acidic Media by N-[(3,4-Dimethoxyphenyl)Methyleneamino]-4-Hydroxy-Benzamide. *J. Bio. Tribo. Corros.* **2021**, *7*, 10.

(7) Thomas, A.; Rugmini Ammal, P.; Joseph, A. A Comprehensive study of mild steel corrosion in the aggressive acidic environment using CMPPC, a substituted pyrazole derivative. *Chem. Pap.* **2020**, *74*, 3025−3037.

(8) Wei, H.; Heidarshenas, B.; Zhou, L.; Li, G.; Hussain, Q.; Ostrikov, K. Green Inhibitors for steel Corrosion in Acidic Environment State-of-art. *Mater. Today Sustain.* **2020**, *10*, 100044.

(9) Verma, C.; Ebenso, E. E.; Quraishi, M. A.; Hussain, C. M. Recent developments in sustainable corrosion inhibitors: design,

performance and industrial scale applications. *Adv. Mater.* **2021**, *2* (12), 3806−3850.
(10) Jayaraman, A.; Mansfeld, F. B.; Wood, T. K. Inhibiting sulfate-reducing bacteria in biofilms by expressing the antimicrobial peptides indolicidin and bactenecin. *J. Indust, Microbiol. Biotechnol.* **1999**, *22*, 167−175.
(11) Rajbir, S.; Debarati, P.; Rakesh, K. J. Biofilms: implications in bioremediation. *Trends. Microbiol.* **2006**, *14*, 389−397.
(12) Ali, J.; Sohail, A.; Wang, L.; Rizwan Haider, M.; Mulk, S.; Pan, G. Electro-microbiology as a promising approach towards renewable energy and environmental sustainability. *Energies.* **2018**, *11*, 1822.
(13) Ding, X.; Yin, B.; Qian, L.; Zeng, Z.; Yang, Z.; Li, H.; Lu, Y.; Zhou, S. Screening for novel quorum-sensing inhibitors to interfere with the formation of Pseudomonas aeruginosa biofilm. *J. Med. Microbiol.* **2011**, *60* (12), 1827−1834.
(14) Sankar Ganesh, P.; Ravishankar Rai, V. Attenuation of quorum-sensing-dependent virulence factors and biofilm formation by medicinal plants against antibiotic resistant Pseudomonas aeruginosa. *J. Trait. Complement. Med.* **2018**, *8* (1), 170−177.
(15) Vasavi, H. S.; Arun, A. B.; Rekha, P. D. Anti-quorum sensing activity of flavonoid-rich from centella asiatica L.against *Pseudomona-saeruginosa* PA01. *J. Microbiol. Immunol. Infect.* **2016**, *49*, 8−15.
(16) de Oliveira, E. S. D.; da C. Pereira, R. F.; de A. Limab, M. G.; Urtiga Filhoa, S. L. Study on Biofilm Forming Microorganisms Associated with the Biocorrosion of X80 Pipeline Steel in Produced Water from Oilfield. *Mater. Res.* **2021**, *24* (6), 20210196.
(17) Jamal, M.; Ahmad, W.; Andleeb, S.; Jalil, F.; Imran, M.; Nawaz, M. A.; Hussain, T.; Ali, M.; Rafiq, M.; Kamil, M. A. Bacterial biofilm and associated infections. *J. Chin. Med. Assoc.* **2018**, *81* (1), 7−11.
(18) (a) Pedersen, A.; Hermansson, M. Inhibition of metal corrosion by bacteria. *Biofouling* **1991**, *3* (1), 1−11. (b) Pedersen, A.; Hermansson, M. The effects on metal corrosion by Serratia marscens and a Pseudomonas sp. *Biofouling.* **1989**, *1*, 313−322.
(19) (a) Jayaraman, A.; Earthman, J. C.; Wood, T. K. Corrosion inhibition by aerobic biofilms on SAE 1018 steel. *Appl. Microbiol. Biotechnol.* **1997**, *47*, 62−68. (b) Garrett, T. R.; Bhakoo, M.; Zhang, Z. Bacterial adhesion and biofilms on surfaces. *Prog. Nat. Sci.* **2008**, *18* (9), 1049−1056.
(20) Tamilselvi, B.; Bhuvaneshwari, D. S.; Padmavathy, S.; Bothi Raja, P. Corrosion inhibition of *Pichia* sp.biofilm against mild steel corrosion in 1M H_2SO_4. *J. Mol. Liquid.* **2022**, *359*, 119359.
(21) Wu, S.; Wang, Y.; Liu, N. A.; Dong, G.; Sheng, C. Tackling fungal resistance by biofilm inhibitors. *J. Med. Chem.* **2017**, *60* (6), 2193−2211.
(22) Bojsen, R. K.; Andersen, K. S.; Regenberg, B. Saccharomyces cerevisiae—a model to uncover molecular mechanisms for yeast biofilm biology. *FEMS. Immunol. Med. Microbiol.* **2012**, *65* (2), 169−182.
(23) Lipke, P. N. What we do not know about fungal cell adhesion molecules. *J. Fungi. Basel. Switz.* **2018**, *4*, 59.
(24) Flemming, H. C.; Wingender, J. The biofilm matrix. *Nat. Rev. Microbiol.* **2010**, *8* (9), 623−633.
(25) Camiolo, S.; Porru, C.; Benítez-Cabello, A.; Rodríguez-Gómez, F.; CaleroDelgado, B.; Porceddu, A.; Budroni, M.; Mannazzu, I.; Jiménez-Díaz, R.; ArroyoLópez, F. N. Genome overview of eight Candida boidinii strains isolated from human activities and wild environments. *Stand. Genom Sci.* **2017**, *12* (1), 70.
(26) Porru, C.; Rodríguez-Gómez, F.; Benítez-Cabello, A.; Jiménez-Díaz, R.; Zara, G.; Budroni, M.; Mannazzu, I.; Arroyo-López, F. N. Genotyping, identification and multifunctional features of yeasts associated to Bosana naturally black table olive fermentations. *Food Microbiol.* **2018**, *69*, 33−42.
(27) Riedl, R.; Fütterer, J.; Goderbauer, P.; et al. Combined yeast biofilm screening— characterization and validation of yeast related biofilms in a brewing environment with combined cultivation and specific real-time PCR screening of selected indicator species. *J. Am. Soc. Brew. Chem.* **2019**, *77*, 99−112.
(28) Aranda, E.; Godoy, P.; Reina, R.; Fabregat, M. B.; Rosell, M.; Marco-Urrea, E.; Romera, I. G. Isolation of Ascomycota fungi with capability to transform PAHs: Insights into the biodegradation mechanisms of Penicillium oxalicum. *Int. Biodeterior. Biodegradation.* **2017**, *122*, 141−150.
(29) Jain, A. Studies on growth parameters and Protein Content of Yeast Saccharomyces cerevisiae on increasing concentration of Lead (Pb). *Int. J. Recent Res.* **2015**, *2*, 46−52.
(30) Villa-Carvajal, M.; Querol, A.; Belloch, C. Identification of species in the genus Pichia by restriction of the internal transcribed spacers (ITS1 and ITS2) and the 5.8S ribosomal DNA gene, Identification of Pichia species by 5.8S-ITS rDNA RFLP. *ALJMAO.* **2006**, *90*, 171−181.
(31) Kim, H. S.; Park, H. D. Ginger extract inhibits biofilm formation by Pseudomonas aeruginosa PA14. *PLoS One* **2013**, *8* (9), No. e76106.
(32) Li, Z.; Zhou, J.; Yuan, X.; Xu, Y.; Xu, D.; Zhang, D.; Feng, D.; Wang, F. Marine Biofilms with Significant Corrosion Inhibition Performance by Secreting Extracellular Polymeric Substances. *ACS Appl. Mater. Interfaces* **2021**, *13* (39), 47272−47282.
(33) Kumar, L.; Bisen, M.; Harjai, K.; Chhibber, S.; Azizov, S.; Lalhlenmawia, H.; Kumar, D. Advances in Nanotechnology for Biofilm Inhibition. *ACS Omega* **2023**, *8* (24), 21391−21409.
(34) Parrilli, E.; Tutino, M. L.; Marino, G. Biofilm as an Adaptation Strategy to Extreme Conditions. *Rend. Fis. Acc. Lincei.* **2022**, *33*, 527−536.
(35) Chhibber, S.; Bansal, S.; Kaur, S. Disrupting the Mixed-Species Biofilm of Klebsiella Pneumoniae B5055 and *Pseudomonas aeruginosa* PAO Using Bacteriophages Alone or in Combination with Xylitol. *Microbiology.* **2015**, *161*, 1369−1377.
(36) Karuppasamy, P.; Thiruppathi, D.; Sundar, J. V.; Rajapandian, V.; Ganesan, M.; Rajendran, T.; Rajagopal, S.; Nagarajan, N.; Rajendran, P.; Sivasubramanian, V. K. Spectral, Computational, Electrochemical and Antibacterial Studies of Iron(III)-Salen Complexes. *Arabian J. Sci. Eng.* **2015**, *40*, 2945.
(37) Bellut, K.; Krogerus, K.; Arendt, E. K. Lachancea fermentati Strain Isolated From Kombuch: Fundamental Insights, and Practical Application in Low Alcohol Beer Brewing. *Front. Microbiol.* **2020**, *11*, 764.
(38) Guerrini, S.; Mangani, S.; Romboli, Y.; Luti, S.; Pazzagli, L.; Granchi, L. Impact of *Saccharomyces cerevisiae* Strains on Health-Promoting Compounds in wine. *Fermentation.* **2018**, *4* (2), 26.
(39) Ma, Y.; Li, Y.; Wang, F. The atmospheric corrosion kinetics of low carbon steel in a tropical marine environment. *Corros. Sci.* **2010**, *52*, 1796−1800.
(40) Suh, S. O.; Blackwell, M.; Kurtzman, C. P.; Lachance, M. A. Phylogenetics of Saccharomycetales, the ascomycete yeasts. *Mycologia.* **2006**, *98* (6), 1006−1017.
(41) Guillemot, G.; Vaca-Medina, G.; Martin-Yken, H.; Vernhet, A.; Schmitz, P.; Mercier-Bonin, M. Shear-flow induced detachment of Saccharomyces cerevisiae from stainless steel: Influence of yeast and solid surface properties. *Colloids Surf.B* **2006**, *49* (2), 126−135.
(42) Yuma, Y. S. Isolation and characterization of yeast as potential probiotics from fermented cereals dough. *J. Vet. Med. Res.* **2020**, *7*, 1202.
(43) Fouda, A. S.; Megahed, H. E.; Fouad, N.; Elbahrawi, N. M. Corrosion inhibition of carbon steel in 1M hydrochloric acid solution by aqueous extract of thevetia peruviana. *J. Bio-Tribo-Corros.* **2016**, *2*, 16.
(44) Fatima Saifee, K.; Filmwala Zoeb, A.; Hussain Kaneez, F. Corrosion Inhibition of Thiourea with Synergistic Effect of Potassium Iodide on Mild steel in Brackish Water and Effluent Water. *Res. J. Chem. Environ.* **2019**, *23*, 6−12.
(45) Becke, A. D. Density Functional Thermochemistry. III. The Role of Exact Exchange. *J. Chem. Phys.* **1993**, *98*, 5648−5652.
(46) Lee, C.; Yang, W.; Parr, R. C. Development of the ColleSalvetti Correlation energy formula into a functional of the electron density. *Phys. Rev. B* **1988**, *37*, 785−789.
(47) Vosko, S. H.; Wilk, L.; Nusair, M. Accurate spin-dependent electron liquid correlation energies for local spin density calculations: a critical analysis. *Can. J. Phys.* **1980**, *58*, 1200−1211.

https://doi.org/10.1021/acsphyschemau.3c00055
ACS Phys. Chem Au 2024, 4, 67−84

(48) Hay, J.; Wadt, W. R. Ab initio effective core potentials for molecular calculations, potentials for K to AU including the outermost core orbitals. *J. Chem. Phys.* **1985**, *82*, 270−283.
(49) Bhuvaneshwari, D. S.; Padmavathy, S.; Tamilselvi, B.; Bothi Raja, P. *Ailanthusexcelsa* as biogenic inhibitor for mild steel corrosion in 0.5M H_2SO_4 medium and antifoultant against fouling bacteria. *Mater. Today Commun.* **2021**, *28*, 102461.
(50) Hatami-manesh, M.; Younesi, H.; Bahramifar, N.; Mohammadi, M.; Khakpour, H. Fermentative production of ethanol from acid hydrolyzate of rice water waste using Saccharomyces cerevisiae: Experimental and kinetic studies. *Waste and Biomass Valorization.* **2020**, *11*, 3465−3475.
(51) Bouklah, M.; Benchat, N.; Hammouti, B.; Aouniti, A.; Kertit, S. Thermodynamic characterisation of steel corrosion and inhibitor adsorption of pyridazine compounds in 0.5 M H_2SO_4. *Mater. Lett.* **2006**, *60*, 1901−1905.
(52) Tang, L.; Mu, G.; Liu, G. The effect of neutral red on the corrosion inhibition of cold rolled steel in 1.0 M hydrochloric acid. *Corros. Sci.* **2003**, *45*, 2251−2262.
(53) Li, X.; Mu, G. Tween-40 as corrosion inhibitor for cold rolled steel in sulphuric acid: Weight loss study, electrochemical characterization, and AFM. *Appl. Surf. Sci.* **2005**, *252*, 1254−1265.
(54) Karthick, K. A.; Bhuvaneshwari, D. S.; Umapathi, D.; Bothi Raja, P. Benign approach of Canthium Parviflorum as a bioinhibitor for mild steel corrosion in 0.5 M H_2SO_4 medium. *Surf. Rev. Lett.* **2020**, *27* (9), 1950208.
(55) Tamil selvi, B.; Bhuvaneshwari, D. S.; Padmavathy, S.; Bothi Raja, P. Corrosion inhibition of *Pichia* sp.biofilm against mild steel corrosion in 1M H_2SO_4. *J. Mol. Liquid.* **2022**, *359*, 119359.
(56) Padmavathy, S.; Tamilselvi, B.; Chen, S.-M.; Bhuvaneshwari, D. S.; Chen, T.-W. Sustainable approach to the antifouling and corrosion inhibitive properties of Exopolysaccharide producing Rhizobium leguminosarum (Legume Root Nodule Associated Bacteria) on mild steel at low pH. *Int. J. Electrochem. Sci.* **2021**, *16*, 210373.
(57) Farahati, R.; Ghaffarinejad, A.; Mousavi-Khoshdel, S. M.; Rezania, J.; Behzadi, H.; Shockravi, A. Synthesis and potential applications of some thiazoles as corrosion inhibitor of copper in 1 M HCl: Experimental and theoretical studies. *Prog. Org. Coat.* **2019**, *132*, 417−428.
(58) Pourghasemi Hanza, A.; Naderi, R.; Kowsari, E.; Sayebani, M. Corrosion behavior of mild steel in H_2SO_4 solution with 1,4-di [1′-methylene-3′-methyl imidazolium bromide]-benzene as an ionic liquid. *Corros. Sci.* **2016**, *107*, 96−106.
(59) Ganapathi Sundaram, R.; Vengatesh, G.; Sundaravadivelu, M. Surface morphological and quantum chemical studies of some expired drug molecules as potential corrosion inhibitors for mild steel in chloride medium. *Surf. Interfaces.* **2021**, *22*, 100841.
(60) Flores, E. A.; Olivares, O.; Likhanova, N. V.; Dominguez-Aguilar, M. A.; Nava, N.; Guzman-Lucero, D.; Corrales, M. Sodium phthalamates as corrosion inhibitors for carbon steel in aqueous hydrochloric acid solution. *Corros. Sci.* **2011**, *53*, 3899−3913.
(61) Parthipan, P.; Sabarinathan, D.; Angaiah, S.; Rajasekar, A. Glycolipid biosurfactant as an eco-friendly microbial inhibitor for the corrosion of carbon steel in vulnerable corrosive bacterial strains. *J.Mol. Liquid.* **2018**, *261*, 473−479.
(62) Freitas, F.; Alves, V. D.; Carvalheira, M.; Costa, N.; Oliveira, R.; Reis, M. A. Emulsifying behaviour and rheological properties of the extracellular polysaccharide produced by Pseudomonas oleovorans grown on glycerol by product. *Carbohydr. Polym.* **2009**, *78*, 549−55.
(63) San-Blas, E.; Cubillán, N.; Guerra, M.; Portillo, E.; Esteves, I. Characterization of *Xenorhabdus* and *Photorhabdus* bacteria by Fourier transform mid-infrared spectroscopy with attenuated total reflection (FT-IR/ATR). *Spectrochim Acta A* **2012**, *93*, 58−62.
(64) Boukhelata, N.; Taguett, F.; Kaci, Y. Characterization of an extracellular polysaccharide produced by a Saharan bacterium Paenibacillus tarimensis REG 0201M. *Ann. Microbiol.* **2019**, *69*, 93−106.
(65) Kalaiselvi, K.; Chung, I.-M.; Kim, S.-H.; Prabakaran, M. Corrosion resistance of mild steel in sulphuric acid solution by Coreopsis tinctoria extract: electrochemical and surface studies. *Anti Corrosion. Meth. Mater.* **2018**, *65* (4), 408−416.
(66) Prabakaran, M.; Kim, S. H.; Mugila, N.; Hemapriya, V.; Parameswari, K.; Chitra, S.; Chung, I. M. Aster koraiensis as nontoxic corrosion inhibitor for mild steel in sulfuric acid. *J. Ind. Eng. Chem.* **2017**, *52*, 235−242.
(67) Bhuvaneshwari, B.; Selvaraj, A.; Iyer, N. R.; Ravikumar, L.; Rai, P. K.; Mondal, K.; Gupta, R. K. Electrochemical and microstructural analysis of azomethine polyamides as inhibitor for rebar corrosion under chloride contaminated pore solution. *Front. Res. Today* **2018**, *1*, 1004.
(68) Verma, D. K.; Al Fantazi, A.; Verma, C.; Khan, F.; Asatkar, A.; Hussain, C. M.; Ebenso, E. E. Experimental and computational studies on hydroxamic acids as environmental friendly chelating corrosion inhibitors for mild steel in aqueous acidic medium. *J. Mol. Liq.* **2020**, *314*, 113651.
(69) Abd El-Lateef, H. M. Corrosion inhibition characteristics of a novel salycilidene isatin hydrazine sodium sulfonate on carbon steel in HCl and a synergistic nickel ions additive: a combined experimental and theoretical perspective. *Appl. Surf. Sci.* **2020**, *501*, 144237.
(70) Li, Z.; Zhou, J.; Yuan, X.; Xu, Y.; Xu, D.; Zhang, D.; Feng, D.; Wang, F. Marine Biofilms with Significant Corrosion Inhibition Performance by Secreting Extracellular Polymeric Substances. *ACS Appl. Mater. Interfaces.* **2021**, *13* (39), 47272−47282.
(71) Prabakaran, M.; Kim, S.-H.; Sasireka, A.; Hemapriya, V.; Chung, I.-M. *β*-Sitosterol isolated from rice hulls as an efficient corrosion inhibitor for mild steel in acidic environments. *New. J. Chem.* **2017**, *41* (10), 3900−3907.
(72) Chung, I. M.; Malathy, R.; Kim, S. H.; Kalaiselvi, K.; Prabakaran, M.; Gopiraman, M. Ecofriendly green inhibitor from Hemerocallis fulva against aluminum corrosion in sulphuric acid medium. *J. Adhes. Sci. Technol.* **2020**, *34*, 1483−1506.
(73) Shrivastava, A.; Pal, M.; Sharma, R. K. Simultaneous Production of Bioethanol and Bioelectricity in a Membrane Less Single chambered Yeast Fuell cell by Saccharomycescerevisiae and Pichiafermentans. *Arab. J. Sci. Eng.* **2022**, *47*, 6763−6771.
(74) Karthick, K. A.; Kaleeswari, K.; Uma Maheswari, C.; Sivaraman, G.; Shankar, B.; Tamilselvi, A. J. Novel pyridoxal based molecular sensor for selective turn-on fluorescent switching functionality towards Zn(II) in live cells. *Photochem. Photobiol. A: Chem.* **2022**, *428*, 113861.
(75) Sghyar, R.; Sert, Y.; Ibrahimi, B. E.; Moussaoui, O.; Hadrami, E. M. E.; Ben-Tama, A.; Mague, J. T.; Talbaoui, A.; Sebbar, N. K.; Essassi, E. M. New tetrazoles compounds incorporating galactose moiety: Synthesis, crystal structure, spectroscopic characterization, Hirshfeld surface analysis, molecular docking studies, DFT calculations and anti-corrosion property anticipation. *J. Mol. Struct.* **2022**, *1247*, 131300.

https://doi.org/10.1021/acsphyschemau.3c00055
ACS Phys. Chem Au 2024, 4, 67−84